JHEP

Published for SISSA by Springer

Received: August 6, 2015
Accepted: September 25, 2015
Published: November 5, 2015

$K^+ \to \pi^+ \nu\bar{\nu}$ and $K_L \to \pi^0 \nu\bar{\nu}$ in the Standard Model: status and perspectives

Andrzej J. Buras, Dario Buttazzo, Jennifer Girrbach-Noe and Robert Knegjens

TUM Institute for Advanced Study,
Lichtenbergstr. 2a, D-85748 Garching, Germany
Physik Department, Technische Universität München,
James-Franck-Straße, D-85748 Garching, Germany

E-mail: andrzej.buras@tum.de, dario.buttazzo@tum.de, jennifer.girrbach@tum.de, robert.knegjens@tum.de

Abstract: In view of the recent start of the NA62 experiment at CERN that is expected to measure the $K^+ \to \pi^+ \nu\bar{\nu}$ branching ratio with a precision of 10%, we summarise the present status of this promising decay within the Standard Model (SM). We do likewise for the closely related $K_L \to \pi^0 \nu\bar{\nu}$, which will be measured by the KOTO experiment around 2020. As the perturbative QCD and electroweak corrections in both decays are under full control, the dominant uncertainties within the SM presently originate from the CKM parameters $|V_{cb}|$, $|V_{ub}|$ and γ. We show this dependence with the help of analytic expressions as well as accurate interpolating formulae. Unfortunately a clarification of the discrepancies between inclusive and exclusive determinations of $|V_{cb}|$ and $|V_{ub}|$ from tree-level decays will likely require results from the Belle II experiment available at the end of this decade. Thus we investigate whether higher precision on both branching ratios is achievable by determining $|V_{cb}|$, $|V_{ub}|$ and γ by means of other observables that are already precisely measured. In this context ε_K and $\Delta M_{s,d}$, together with the expected progress in QCD lattice calculations will play a prominent role. We find $\mathcal{B}(K^+ \to \pi^+ \nu\bar{\nu}) = (9.11 \pm 0.72) \times 10^{-11}$ and $\mathcal{B}(K_L \to \pi^0 \nu\bar{\nu}) = (3.00 \pm 0.30) \times 10^{-11}$, which is more precise than using averages of the present tree-level values of $|V_{cb}|$, $|V_{ub}|$ and γ. Furthermore, we point out the correlation between $\mathcal{B}(K^+ \to \pi^+ \nu\bar{\nu})$, $\overline{\mathcal{B}}(B_s \to \mu^+ \mu^-)$ and γ within the SM, that is only very weakly dependent on other CKM parameters. Finally, we update the correlation of $K_L \to \pi^0 \nu\bar{\nu}$ with the ratio ε'/ε in the SM taking the recent progress on ε'/ε from lattice QCD and the large N approach into account.

Keywords: Rare Decays, Kaon Physics, Standard Model

ArXiv ePrint: 1503.02693

doi:10.1007/JHEP11(2015)033

JHEP11(2015)033

Contents

1 Introduction 1

2 Basic formulae 4
- 2.1 $K^+ \to \pi^+ \nu\bar{\nu}$ 4
- 2.2 $K_L \to \pi^0 \nu\bar{\nu}$ 6
- 2.3 Experimental prospects 6

3 CKM inputs from tree-level observables 7
- 3.1 Determination of the branching ratios 7
- 3.2 Correlations between observables 10

4 CKM inputs from loop-level observables 14

5 The ratio ε'/ε in the Standard Model 20

6 Summary and outlook 23

A Expression for X_t 24

B Expression for $P_c(X)$ 25

C More details on ε'/ε 26

JHEP11(2015)033

1 Introduction

The measurements of the branching ratios of the two *golden* modes $K^+ \to \pi^+ \nu\bar{\nu}$ and $K_L \to \pi^0 \nu\bar{\nu}$ will be among the top highlights of flavour physics in the rest of this decade. $K^+ \to \pi^+ \nu\bar{\nu}$ is CP conserving while $K_L \to \pi^0 \nu\bar{\nu}$ is governed by CP violation. Both decays are dominated in the SM and in many of its extensions by Z penguin diagrams. These decays are theoretically very clean, and the calculation of their branching ratios within the SM includes next-to-leading order (NLO) QCD corrections to the top quark contributions [1–3], NNLO QCD corrections to the charm contribution [4–6] and NLO electroweak corrections [7–9] to both top and charm contributions. Moreover, extensive calculations of isospin breaking effects and non-perturbative effects have been performed [10, 11]. Reviews of these two decays can be found in [12–18] and their power in probing energy scales as high as several hundreds of TeV has been demonstrated in [19].

In view of the recent start of the NA62 experiment at CERN that is expected to measure the $K^+ \to \pi^+ \nu\bar{\nu}$ branching ratio with a precision of 10% compared to the SM prediction [20, 21], and the expected measurement of $K_L \to \pi^0 \nu\bar{\nu}$ by KOTO around 2020

at J-PARC [15, 22], it is the right time to summarise the present status of these decays within the SM. This is motivated in particular by the fact that different estimates appear in the literature due to different inputs used for the Cabibbo-Kobayashi-Maskawa (CKM) matrix elements, which presently constitute the main uncertainty in the SM predictions for these two branching ratios. This has been stressed in [23], where the dependence of both branching ratios on the chosen values of $|V_{cb}|$ and $|V_{ub}|$ extracted from tree-level decays has been studied (see table 3 of that paper).

At this point two strategies for the determination of the contribution of the SM dynamics to these decays are envisaged:

Strategy A: the CKM matrix is determined using tree-level measurements of

$$|V_{us}|, \qquad |V_{cb}|, \qquad |V_{ub}|, \qquad \gamma, \tag{1.1}$$

where γ is an angle of the unitarity triangle (UT). As New Physics (NP) seems to now be well separated from the electroweak scale, this determination of the CKM matrix is not expected to be polluted by NP contributions.[1] Inserting these inputs into the known expressions for the relevant branching ratios (see section 2) then allows a determination of the SM values for the $K \to \pi\nu\bar{\nu}$ branching ratios independently of whether NP is present at short distance scales or not. The departure of these predictions from future data would therefore allow us to discover whether NP contributes to these decays independently of whether it contributes to other decays or not. This information is clearly important for the selection of successful extensions of the SM through flavour-violating processes.

Unfortunately, this strategy cannot be executed in a satisfactory manner at present due to the discrepancies between inclusive and exclusive determinations of $|V_{cb}|$ and $|V_{ub}|$ from tree-level decays. Moreover, the precision on γ from tree-level decays is still unsatisfactory for this purpose. While the measurement of γ should be significantly improved by LHCb in the coming years, discrepancies between inclusive and exclusive determinations of $|V_{cb}|$ and $|V_{ub}|$ from tree-level decays are likely to be resolved only by the time of the Belle II experiment at SuperKEKB at the end of this decade.

The clarification of the discrepancies between inclusive and exclusive determinations of $|V_{cb}|$ and $|V_{ub}|$ from tree-level decays is important, but there are reasons to expect that the exclusive determinations will eventually be the ones to be favoured. First of all, exclusive measurements are easier to perform than the inclusive ones. Equally important, due to the significant improvement in the calculations of the relevant form factors by lattice QCD, exclusive determinations are more straightforward than the inclusive ones. This is opposite to the philosophy of ten years ago, where QCD lattice calculations were still at the early stage and inclusive determinations were favoured.

Yet, from the present perspective it is useful to study the SM predictions for $K^+ \to \pi^+\nu\bar{\nu}$ and $K_L \to \pi^0\nu\bar{\nu}$ in the full range of $|V_{cb}|$, $|V_{ub}|$ and γ known from tree-level decays, as this will clearly demonstrate the need for the reduction of parametric uncertainties. This will also allow the SM predictions for these decays to be monitored as the determination of

[1] Recent analyses of the room left for NP in tree-level decays can be found in [24–26].

JHEP11(2015)033

γ will improve in the coming years at the LHC. This should be of interest in view of the first results on $K^+ \to \pi^+\nu\bar{\nu}$ from NA62, which are expected already in 2016. Moreover, it will also be of interest to see how other observables, like ε_K, ΔM_s, ΔM_d, and rare $B_{s,d}$ decays are modified when the parameters in (1.1) are varied, and what their correlations with $K^+ \to \pi^+\nu\bar{\nu}$ and $K_L \to \pi^0\nu\bar{\nu}$ are within the SM. As we will see, some of these correlations are practically independent of $|V_{cb}|$ and $|V_{ub}|$ and as such are particularly suited for a precise tests of the SM.

Strategy B: here the assumption is made that the SM is the whole story and all available information from flavour-changing neutral current (FCNC) processes is used to determine the CKM matrix. Our strategy here will be to ignore tree-level determinations of $|V_{ub}|$ and $|V_{cb}|$, as the discrepancies mentioned above could also result from experimental data, which will improve only at the end of this decade. Similarly, the tree-level determination of γ will be left out. Then the observables to be used for the determination of the CKM parameters will be [2]

$$\varepsilon_K, \qquad \Delta M_s, \qquad \Delta M_d, \qquad S_{\psi K_S}, \tag{1.2}$$

accompanied by lattice QCD calculations of the relevant non-perturbative parameters. In this manner also $|V_{cb}|$, $|V_{ub}|$ and γ can be determined. This is basically what the UTfit [27] and CKMfitter [28] collaborations do, except that we ignore the tree-level determinations of $|V_{cb}|$, $|V_{ub}|$ and γ for the reasons stated above. As the dominant top quark contribution to ε_K is proportional to $|V_{cb}|^4$ and $\Delta M_{s,d}$ are proportional to $|V_{cb}|^2$, a useful determination of $|V_{cb}|$ can be obtained from these quantities.[3] The full UT is then constructed by using the ratio $\Delta M_d/\Delta M_s$ and $S_{\psi K_S}$. We find that with the most recent lattice QCD input on the parameter ξ [31], the determination of γ in this manner is impressive, and also the value of $|V_{cb}|$ is significantly more accurate than from tree-level decays. In the case of $|V_{ub}|$ the accuracy is found to be comparable to the most recent exclusive determination [32].

It should be emphasised that while strategy A is ultimately the one to use to study extensions of the SM, the virtue of strategy B at present is the greater accuracy of the SM predictions for the observables that we consider. By simply imposing constraints from several measurements we arrive at narrow ranges for the parameters in (1.1) — given that the SM is the whole story.

In the present paper we will follow these two strategies using the most recent inputs relevant for both of them, in particular the ones from lattice QCD. In section 2 we summarise the present status of the $K^+ \to \pi^+\nu\bar{\nu}$ and $K_L \to \pi^0\nu\bar{\nu}$ decays in the SM and discuss the main uncertainties with the help of analytic expressions. In sections 3 and 4 we follow strategies A and B, respectively, and present in some detail our numerical results. In section 5 we present an updated analysis of the correlation of $K_L \to \pi^0\nu\bar{\nu}$ and the ratio ε'/ε in the SM. We conclude in section 6. In the appendices we collect a number of additional expressions that we used in our analysis.

[2] Note that the present determination of $S_{\psi\phi}$ has no impact on the CKM parameters in the SM.

[3] The strategy for the determination of $|V_{cb}|$ from ε_K is not new [29] and has been considered recently in [30]. See in particular formula (29) in that paper.

JHEP11(2015)033

2 Basic formulae

We present here the basic formulae for the branching ratios for the $K^+ \to \pi^+\nu\bar{\nu}$ and $K_L \to \pi^0\nu\bar{\nu}$ decays in the SM. This section can be considered as an update to the analogous section (section 2) of [12], a review of these decays from 2007. The main advances in the last eight years are:

- computation of complete NLO electroweak corrections to the charm quark contribution to $K^+ \to \pi^+\nu\bar{\nu}$ in [7];
- computation of complete NLO electroweak corrections to the top quark contribution to $K^+ \to \pi^+\nu\bar{\nu}$ and $K_L \to \pi^0\nu\bar{\nu}$ in [8];
- reduction of uncertainties due to $m_t(m_t)$, $m_c(m_c)$ and $\alpha_s(M_Z)$, with the last two relevant in particular for the charm contribution to $K^+ \to \pi^+\nu\bar{\nu}$.

While incorporating these advances in our presentation we will also include

- NLO QCD corrections to the top quark contributions [1–3] and NNLO QCD corrections to the charm contribution [4–6];
- isospin breaking effects and non-perturbative effects [10, 11].

2.1 $K^+ \to \pi^+\nu\bar{\nu}$

The branching ratio for $K^+ \to \pi^+\nu\bar{\nu}$ in the SM is dominated by Z^0 penguin diagrams, with a significant contribution from box diagrams. Summing over three neutrino flavours, it can be written as follows [3, 11]

$$\mathcal{B}(K^+ \to \pi^+\nu\bar{\nu}) = \kappa_+(1+\Delta_{\rm EM})\cdot\left[\left(\frac{{\rm Im}\lambda_t}{\lambda^5}X(x_t)\right)^2 + \left(\frac{{\rm Re}\lambda_c}{\lambda}P_c(X) + \frac{{\rm Re}\lambda_t}{\lambda^5}X(x_t)\right)^2\right], \tag{2.1}$$

with

$$\kappa_+ = (5.173 \pm 0.025)\cdot 10^{-11}\left[\frac{\lambda}{0.225}\right]^8, \qquad \Delta_{\rm EM} = -0.003. \tag{2.2}$$

Here $x_t = m_t^2/M_W^2$, $\lambda = |V_{us}|$, $\lambda_i = V_{is}^* V_{id}$ are the CKM factors discussed below, and κ_+ summarises the remaining factors, in particular the relevant hadronic matrix elements that can be extracted from leading semi-leptonic decays of K^+, K_L and K_S mesons [11]. $\Delta_{\rm EM}$ describes the electromagnetic radiative correction from photon exchanges. $X(m_t)$ and $P_c(X)$ are the loop functions for the top and charm quark contributions, which are discussed below. An explicit derivation of (2.1) can be found in [33]. The apparent large sensitivity of $\mathcal{B}(K^+ \to \pi^+\nu\bar{\nu})$ to λ is spurious as $P_c(X) \sim \lambda^{-4}$ (see (2.6)) and the dependence on λ in (2.2) cancels the one in (2.1) to a large extent. Therefore when changing λ it is essential to keep track of all the λ dependence.

JHEP11(2015)033

In obtaining the numerical values in (2.2) [11], the $\overline{\rm MS}$ scheme with

$$\sin^2\theta_w(M_Z) = 0.23116, \qquad \alpha(M_Z) = \frac{1}{127.925}, \tag{2.3}$$

has been used. As their errors are below 0.1% these can currently be neglected. Note, however, that although the prefactor of the effective Hamiltonian, $\alpha/\sin^2\theta_w$, is precisely known in a particular renormalisation scheme ($\overline{\rm MS}$ in this case) it remains a scheme dependent quantity, with the scheme dependence only removed by considering higher order electroweak effects in $K \to \pi\nu\bar{\nu}$. An analysis of such effects in the large m_t limit [9] demonstrated that in principle this scheme dependence could introduce a $\pm 5\%$ correction in the $K \to \pi\nu\bar{\nu}$ branching ratios, and that with the $\overline{\rm MS}$ definition of $\sin^2\theta_W$ these higher order electroweak corrections are found below 2%. However, only the complete analysis of two-loop electroweak contributions to $K \to \pi\bar{\nu}\nu$ in [8] for the top contribution could put such expectations on firm footing. The same applies to the NLO electroweak effects in the charm contribution to $K^+ \to \pi^+\nu\bar{\nu}$ evaluated in [7].

The short distance function $X(x_t)$ relevant for the top quark contribution, including NLO QCD corrections [1–3] and two-loop electroweak contributions [8], is

$$X(x_t) = 1.481 \pm 0.005_{\rm th} \pm 0.008_{\rm exp}, \tag{2.4}$$

where the first error comes from the remaining renormalisation scale and scheme uncertainties, as well as the theoretical error on the $\overline{\rm MS}$ parameters due to the matching at the electroweak scale, while the second one corresponds to the combined experimental error on the top and W masses entering the ratio x_t, and on the strong coupling $\alpha_s(M_Z)$. The central value and errors in (2.4) have been obtained using the $\overline{\rm MS}$ couplings with full NNLO precision [34] — 3-loop running in the SM and 2-loop matching at the weak scale (plus 4-loop QCD running of α_s and 3-loop QCD matching in α_s and y_t) — and varying the renormalisation scale between $M_t/2$ and $2M_t$. The NLO EW correction has been included, using the result presented in [8], in order to eliminate the large EW renormalisation scheme dependence of the pure QCD result. See appendix A for details about the different contributions to $X(x_t)$.

The parameter $P_c(X)$ summarises the charm contribution and is defined through

$$P_c(X) = P_c^{\rm SD}(X) + \delta P_{c,u}, \qquad \delta P_{c,u} = 0.04 \pm 0.02, \tag{2.5}$$

with the long-distance contributions $\delta P_{c,u}$ calculated in [10]. Future lattice calculations could reduce the present error in this part [35]. The short-distance part is given by

$$P_c^{\rm SD}(X) = \frac{1}{\lambda^4}\left[\frac{2}{3}X_{\rm NNL}^e + \frac{1}{3}X_{\rm NNL}^\tau\right] \tag{2.6}$$

where the functions $X_{\rm NNL}^\ell$ result from QCD NLO [3, 36] and NNLO calculations [4, 5]. They also include complete two-loop electroweak contributions [7]. The index "ℓ" distinguishes between the charged lepton flavours in the box diagrams. This distinction is irrelevant in the top contribution due to $m_t \gg m_\ell$ but is relevant in the charm contribution as $m_\tau > m_c$.

JHEP11(2015)033

The inclusion of NLO and NNLO QCD corrections have reduced considerably the large dependence on the renormalisation scale μ_c (with $\mu_c = \mathcal{O}(m_c)$) present in the leading order expressions for the charm contribution. The two-loop electroweak corrections on the other hand reduced the dependence on the definition of electroweak parameters. An excellent approximation for $P_c^{\rm SD}(X)$, including all these corrections, as a function of $\alpha_s(M_Z)$ and $m_c(m_c)$ is given in (50) of [7] (see appendix B). Using this formula for the most recent input parameters [37, 38]

$$\lambda = 0.2252(9), \qquad m_c(m_c) = 1.279(13)\,\text{GeV}, \qquad \alpha_s(M_Z) = 0.1185(6) \tag{2.7}$$

we find

$$P_c^{\rm SD}(X) = 0.365 \pm 0.012. \tag{2.8}$$

Adding the long distance contribution in (2.5) we finally find

$$P_c(X) = 0.404 \pm 0.024, \tag{2.9}$$

where we have added the errors in quadratures. We will use this value in our numerical analysis. In obtaining the error in (2.9) we kept λ fixed at its central value, as its error is very small and the strong dependence on λ in $P_c^{\rm SD}(X)$ is canceled by other factors in the formula for the branching ratio as discussed above.

2.2 $K_L \to \pi^0 \nu\bar{\nu}$

The branching ratio for $K_L \to \pi^0 \nu\bar{\nu}$ in the SM is fully dominated by the diagrams with internal top exchanges, with the charm contribution well below 1%. It can be written then as follows [39, 40]

$$\mathcal{B}(K_L \to \pi^0 \nu\bar{\nu}) = \kappa_L \cdot \left(\frac{\text{Im}\lambda_t}{\lambda^5} X(x_t) \right)^2, \tag{2.10}$$

where [11]

$$\kappa_L = (2.231 \pm 0.013) \cdot 10^{-10} \left[\frac{\lambda}{0.225} \right]^8. \tag{2.11}$$

We have summed over three neutrino flavours. An explicit derivation of (2.10) can be found in [33]. Due to the absence of $P_c(X)$ in (2.10), the theoretical uncertainties in $\mathcal{B}(K_L \to \pi^0 \nu\bar{\nu})$ are due only to $X(x_t)$ and amount to about 1% at the level of the branching ratio. The main uncertainty then comes from $\text{Im}\lambda_t$, which is by far dominant with respect to the other parametric uncertainties due to κ_L and m_t, with the latter present in $X(x_t)$.

2.3 Experimental prospects

Experimentally we have [41]

$$\mathcal{B}(K^+ \to \pi^+ \nu\bar{\nu})_{\rm exp} = (17.3^{+11.5}_{-10.5}) \cdot 10^{-11}, \tag{2.12}$$

and the 90% C.L. upper bound [42]

$$\mathcal{B}(K_L \to \pi^0 \nu\bar{\nu})_{\rm exp} \leq 2.6 \cdot 10^{-8}. \tag{2.13}$$

JHEP11(2015)033

The prospects for improved measurements of $\mathcal{B}(K^+ \to \pi^+\nu\bar{\nu})$ are very good. One should stress that already a measurement of this branching ratio with an accuracy of 10% will give us a very important insight into the physics at short distance scales. Indeed the NA62 experiment at CERN [20, 21] is aiming to reach this precision, and it is expected to accumulate 100 SM events with a good signal over background figure by 2018. In order to achieve a 5% measurement of the branching ratio, which will be the next goal of NA62, more time is needed. The planned new experiment at Fermilab (ORKA) could in principle reach the accuracy of 5% [43].[4]

Concerning $K_L \to \pi^0\nu\bar{\nu}$, the KOTO experiment at J-PARC aims in the first step in measuring $\mathcal{B}(K_L \to \pi^0\nu\bar{\nu})$ at SM sensitivity and should provide interesting results around 2020 on this branching ratio [15, 22]. There are also plans to measure this decay at CERN and one should hope that Fermilab will contribute to these efforts in the next decade. The combination of $K^+ \to \pi^+\nu\bar{\nu}$ and $K_L \to \pi^0\nu\bar{\nu}$ is particularly powerful in testing NP. Assuming that NA62 and KOTO will reach the expected precision and the branching ratios on these decays will be at least as high as the ones predicted in the SM, these two decays are expected to be the superstars of flavour physics after 2018.

3 CKM inputs from tree-level observables

3.1 Determination of the branching ratios

As discussed in the introduction, the CKM matrix can be determined by the tree-level measurements $|V_{ub}|$, $|V_{cb}|$, $|V_{us}|$, and the angle γ of the UT. Although this is in principle the optimal strategy, it is currently marred by disagreements between the exclusive and inclusive determinations of both $|V_{ub}|$ and $|V_{cb}|$ — for recent reviews see [53–55]. We proceed to present the latest results of both determinations, as well as our weighted average, with which we will give the SM predictions in what we call strategy A.

The most recent exclusive determinations from lattice QCD form factors are [32, 44, 56]

$$|V_{ub}|_{\rm excl} = (3.72 \pm 0.14) \times 10^{-3}, \qquad |V_{cb}|_{\rm excl} = (39.36 \pm 0.75) \times 10^{-3}. \tag{3.1}$$

The inclusive values are given by [44, 57]

$$|V_{ub}|_{\rm incl} = (4.40 \pm 0.25) \times 10^{-3}, \qquad |V_{cb}|_{\rm incl} = (42.21 \pm 0.78) \times 10^{-3}. \tag{3.2}$$

We take a weighted average and scale the errors based on the resulting χ^2 (specifically, we follow the method advocated in [38]), which gives

$$|V_{ub}|_{\rm avg} = (3.88 \pm 0.29) \times 10^{-3}, \qquad |V_{cb}|_{\rm avg} = (40.7 \pm 1.4) \times 10^{-3}. \tag{3.3}$$

For the CKM angle γ we take the current world average of direct measurements [47]

$$\gamma = (73.2^{+6.3}_{-7.0})^\circ. \tag{3.4}$$

Using this, together with $|V_{us}| = \lambda$ already given in (2.7), we can determine the full CKM matrix.

[4] Unfortunately the US P5 committee did not recommend moving ahead with ORKA and it appears that the precision on $\mathcal{B}(K^+ \to \pi^+\nu\bar{\nu})$ will depend in the coming ten years entirely on the progress made by NA62.

JHEP11(2015)033

	exclusive	inclusive	average	measured
$\mathrm{BR}(K^+ \to \pi^+ \nu\bar{\nu})$ $[10^{-11}]$	$7.62^{+0.69}_{-0.70}$	$9.30^{+0.89}_{-0.92}$	$8.39^{+1.06}_{-1.03}$	$17.3^{+11.5}_{-10.5}$
$\mathrm{BR}(K_L \to \pi^0 \nu\bar{\nu})$ $[10^{-11}]$	$2.88^{+0.30}_{-0.35}$	$4.64^{+0.63}_{-0.68}$	$3.36^{+0.60}_{-0.61}$	≤ 2600
$\overline{\mathrm{BR}}(B_s \to \mu^+\mu^-)$ $[10^{-9}]$	$3.18^{+0.18}_{-0.18}$	$3.66^{+0.21}_{-0.20}$	$3.40^{+0.28}_{-0.27}$	2.8 ± 0.7
$\mathrm{BR}(B_d \to \mu^+\mu^-)$ $[10^{-10}]$	$1.00^{+0.11}_{-0.12}$	$1.17^{+0.14}_{-0.14}$	$1.08^{+0.13}_{-0.14}$	$3.6^{+1.6}_{-1.4}$
$\lvert\varepsilon_K\rvert$ $[10^{-3}]$	$1.96^{+0.25}_{-0.27}$	$2.74^{+0.36}_{-0.38}$	$2.23^{+0.35}_{-0.36}$	2.228 ± 0.011
$S^{\mathrm{SM}}_{\psi K_S}$	$0.74^{+0.02}_{-0.03}$	$0.80^{+0.03}_{-0.04}$	$0.75^{+0.05}_{-0.05}$	0.682 ± 0.019
ΔM_s $[\mathrm{ps}^{-1}]$	$16.19^{+2.37}_{-2.23}$	$18.64^{+2.73}_{-2.56}$	$17.34^{+2.74}_{-2.58}$	17.761 ± 0.022
ΔM_d $[\mathrm{ps}^{-1}]$	$0.52^{+0.09}_{-0.09}$	$0.60^{+0.11}_{-0.11}$	$0.55^{+0.10}_{-0.10}$	0.510 ± 0.003
$\mathrm{Im}(\lambda_t)$ $[10^{-4}]$	$1.40^{+0.07}_{-0.09}$	$1.78^{+0.12}_{-0.13}$	$1.51^{+0.13}_{-0.14}$	–
$\mathrm{Re}(\lambda_t)$ $[10^{-4}]$	$-2.99^{+0.19}_{-0.19}$	$-3.39^{+0.24}_{-0.23}$	$-3.20^{+0.29}_{-0.29}$	–
R_b	$0.41^{+0.02}_{-0.02}$	$0.45^{+0.03}_{-0.03}$	$0.41^{+0.03}_{-0.03}$	–

Table 1. Values of $\mathcal{B}(K^+ \to \pi^+\nu\bar{\nu})$, $\mathcal{B}(K_L \to \pi^0\nu\bar{\nu})$ and of other observables within the SM for the three choices of $|V_{ub}|$ and $|V_{cb}|$ following strategy A as discussed in the text.

In particular, we can determine the quantities λ_t and λ_c, which enter the expressions for the branching ratios in (2.1) and (2.10), as functions of these input parameters. These expressions are:

$$\mathrm{Re}\lambda_t \simeq |V_{ub}||V_{cb}|\cos\gamma(1-2\lambda^2) + (|V_{ub}|^2 - |V_{cb}|^2)\lambda\left(1-\frac{\lambda^2}{2}\right), \tag{3.5}$$

$$\mathrm{Im}\lambda_t \simeq |V_{ub}||V_{cb}|\sin\gamma, \tag{3.6}$$

$$\mathrm{Re}\lambda_c \simeq -\lambda\left(1-\frac{\lambda^2}{2}\right), \tag{3.7}$$

which, with respect to their leading order in λ, are accurate up to $\mathcal{O}(\lambda^4)$ corrections. The (exact) numerical values for $\mathrm{Re}\lambda_t$ and $\mathrm{Im}\lambda_t$ obtained from our three different choices of V_{ub} and V_{cb} in (3.1)–(3.3) are given in table 1.

These expressions can then be directly inserted into (2.1) and (2.10) in order to determine the two branching ratios. Using our averages from (3.3) together with (3.4) gives

$$\mathcal{B}(K^+ \to \pi^+\nu\bar{\nu}) = (8.4 \pm 1.0) \times 10^{-11}, \tag{3.8}$$

$$\mathcal{B}(K_L \to \pi^0\nu\bar{\nu}) = (3.4 \pm 0.6) \times 10^{-11}. \tag{3.9}$$

In figure 1 we show the error budgets for these two observables, and see that the CKM uncertainties dominate. In particular in the case of $K^+ \to \pi^+\nu\bar{\nu}$ we observe large uncertainties due to $|V_{cb}|$ and γ, while in the case of $K_L \to \pi^0\nu\bar{\nu}$ the uncertainty due to $|V_{ub}|$

JHEP11(2015)033

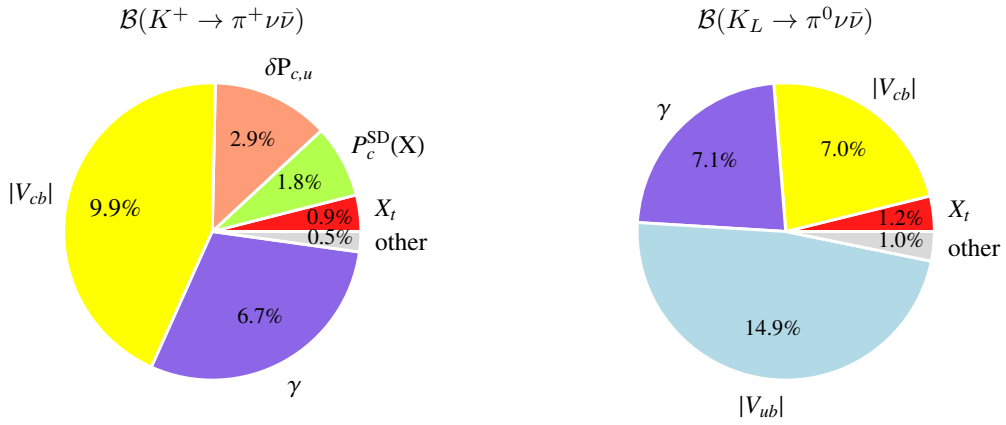

Figure 1. Error budgets for the branching ratio observables $\mathcal{B}(K^+ \to \pi^+\nu\bar{\nu})$ and $\mathcal{B}(K_L \to \pi^0\nu\bar{\nu})$. The remaining parameters, which each contribute an error of less than 1%, are grouped into the "other" category.

dominates but the ones from $|V_{cb}|$ and γ are also large. The remaining parameters, which each contribute an error of less than 1%, are grouped into the "other" category.

For convenience we give the following parametric expressions for the branching ratios in terms of the CKM inputs:

$$\mathcal{B}(K^+ \to \pi^+\nu\bar{\nu}) = (8.39 \pm 0.30) \times 10^{-11} \cdot \left[\frac{|V_{cb}|}{40.7 \times 10^{-3}}\right]^{2.8} \left[\frac{\gamma}{73.2^\circ}\right]^{0.74}, \tag{3.10}$$

$$\mathcal{B}(K_L \to \pi^0\nu\bar{\nu}) = (3.36 \pm 0.05) \times 10^{-11} \cdot \left[\frac{|V_{ub}|}{3.88 \times 10^{-3}}\right]^{2} \left[\frac{|V_{cb}|}{40.7 \times 10^{-3}}\right]^{2} \left[\frac{\sin(\gamma)}{\sin(73.2^\circ)}\right]^{2}. \tag{3.11}$$

The parametric relation for $\mathcal{B}(K_L \to \pi^0\nu\bar{\nu})$ is exact, while for $\mathcal{B}(K^+ \to \pi^+\nu\bar{\nu})$ it gives an excellent approximation: for the large ranges $37 \le |V_{cb}| \times 10^3 \le 45$ and $60^\circ \le \gamma \le 80^\circ$ it is accurate to 1% and 0.5%, respectively. In the case of $\mathcal{B}(K^+ \to \pi^+\nu\bar{\nu})$ we have absorbed $|V_{ub}|$ into the non-parametric error due to the weak dependence on it. The exact dependence of both branching ratios on $|V_{ub}|$, $|V_{cb}|$ and γ is shown in figure 2.

In order to obtain the values of ε_K, $S_{\psi K_S}$, $\Delta M_{s,d}$ and of the branching ratios for $B_{s,d} \to \mu^+\mu^-$ we use the known expressions collected in [16], together with the parameters listed in table 2. The "bar" on the $B_s \to \mu^+\mu^-$ branching ratio, $\overline{\mathcal{B}}(B_s \to \mu^+\mu^-)$, denotes an average over the two mass-eigenstates, as measured by experiment, rather than an average over the two flavour-states, which differs in the B_s system [58–60].

In table 1 we show the results for the $K^+ \to \pi^+\nu\bar{\nu}$ and $K_L \to \pi^0\nu\bar{\nu}$ branching ratios and other observables, for three choices of the pair $(|V_{ub}|, |V_{cb}|)$ corresponding to the exclusive determination (3.1), the inclusive determination (3.2) and our average (3.3). We use (3.4) for γ in each case. We observe:

- The uncertainty in $\mathcal{B}(K^+ \to \pi^+\nu\bar{\nu})$ amounts to more than 10% and has to be decreased to compete with future NA62 measurements, but finding this branching ratio in the ballpark of 15×10^{-11} would clearly indicate NP at work.

JHEP11(2015)033

$\lvert\epsilon_K\rvert$	$2.228(11)\times10^{-3}$	[38]	F_K	156.1(11) MeV	[44]
$S_{\psi K_S}$	0.682(19)	[45]	$\hat{B}_K$	0.750(15)	[44, 46]
ΔM_K	$0.5292(9)\times10^{-2}\,\text{ps}^{-1}$	[38]	F_{B_d}	190.5(42) MeV	[44]
ΔM_d	$0.507(4)\,\text{ps}^{-1}$	[45]	F_{B_s}	227.7(45) MeV	[44]
ΔM_s	$17.761(22)\,\text{ps}^{-1}$	[45]	$F_{B_s}\sqrt{\hat{B}_{B_s}}$	266(18) MeV	[44]
γ	$\left(73.2^{+6.3}_{-7.0}\right)^\circ$	[47]	ξ	1.268(63)	[44]
$\lvert V_{us}\rvert$	0.2252(9)	[45]			
$\Delta\Gamma_s/\Gamma_s$	0.138(12)	[45]	η_{cc}	1.87(76)	[48]
τ_{B_d}	1.519(5) ps	[45]	η_{ct}	0.496(47)	[49]
τ_{B_s}	1.512(7) ps	[45]	η_{tt}	0.5765(65)	[50]
$\alpha_s(M_Z)$	0.1185(6)	[38]	η_B	0.55(1)	[50, 51]
$m_c(m_c)$	1.279(13) GeV	[37]			
M_t	173.34(82) GeV	[52]			

Table 2. Values of theoretical and experimental quantities used as input parameters.

- On the other hand, consistency with $\overline{\mathcal{B}}(B_s\to\mu^+\mu^-)$ would imply the $K^+\to\pi^+\nu\bar{\nu}$ branching ratio to be in the ballpark of 7×10^{-11}. In such a case the search for NP in this decay will be a real challenge and the simultaneous measurement of $K_L\to\pi^0\nu\bar{\nu}$ will be crucial.

- The values of $S_{\psi K_S}$ are typically above the data but only in the case of the *inclusive* determinations of both $|V_{cb}|$ and $|V_{ub}|$ is a new CP phase required.

- The accuracy on the SM prediction for ΔM_s and ΔM_d is far from being satisfactory. Yet, the prospects of improving the accuracy by a factor of two to three in this decade are good.

3.2 Correlations between observables

Correlations between $K^+\to\pi^+\nu\bar{\nu}$ and $B_q\to\mu^+\mu^-$. From inspection of the formulae for the branching ratios for $K^+\to\pi^+\nu\bar{\nu}$ and $B_{s,d}\to\mu^+\mu^-$, each of which in particular depends on $|V_{cb}|$, we derive the following approximate relations

$$\mathcal{B}(K^+\to\pi^+\nu\bar{\nu}) = (8.39\pm0.58)\times10^{-11}\cdot\left[\frac{\gamma}{73.2^\circ}\right]^{0.81} \times\left[\frac{\overline{\mathcal{B}}(B_s\to\mu^+\mu^-)}{3.4\times10^{-9}}\right]^{1.42}\left[\frac{227.7\,\text{MeV}}{F_{B_s}}\right]^{2.84}, \tag{3.12}$$

$$\mathcal{B}(K^+\to\pi^+\nu\bar{\nu}) = (8.41\pm0.77)\times10^{-11}\cdot\left[\frac{\overline{\mathcal{B}}(B_s\to\mu^+\mu^-)}{3.4\times10^{-9}}\right]^{0.74}\left[\frac{227.7\,\text{MeV}}{F_{B_s}}\right]^{1.48} \times\left[\frac{\mathcal{B}(B_d\to\mu^+\mu^-)}{1.08\times10^{-10}}\right]^{0.72}\left[\frac{190.5\,\text{MeV}}{F_{B_d}}\right]^{1.44}. \tag{3.13}$$

JHEP11(2015)033

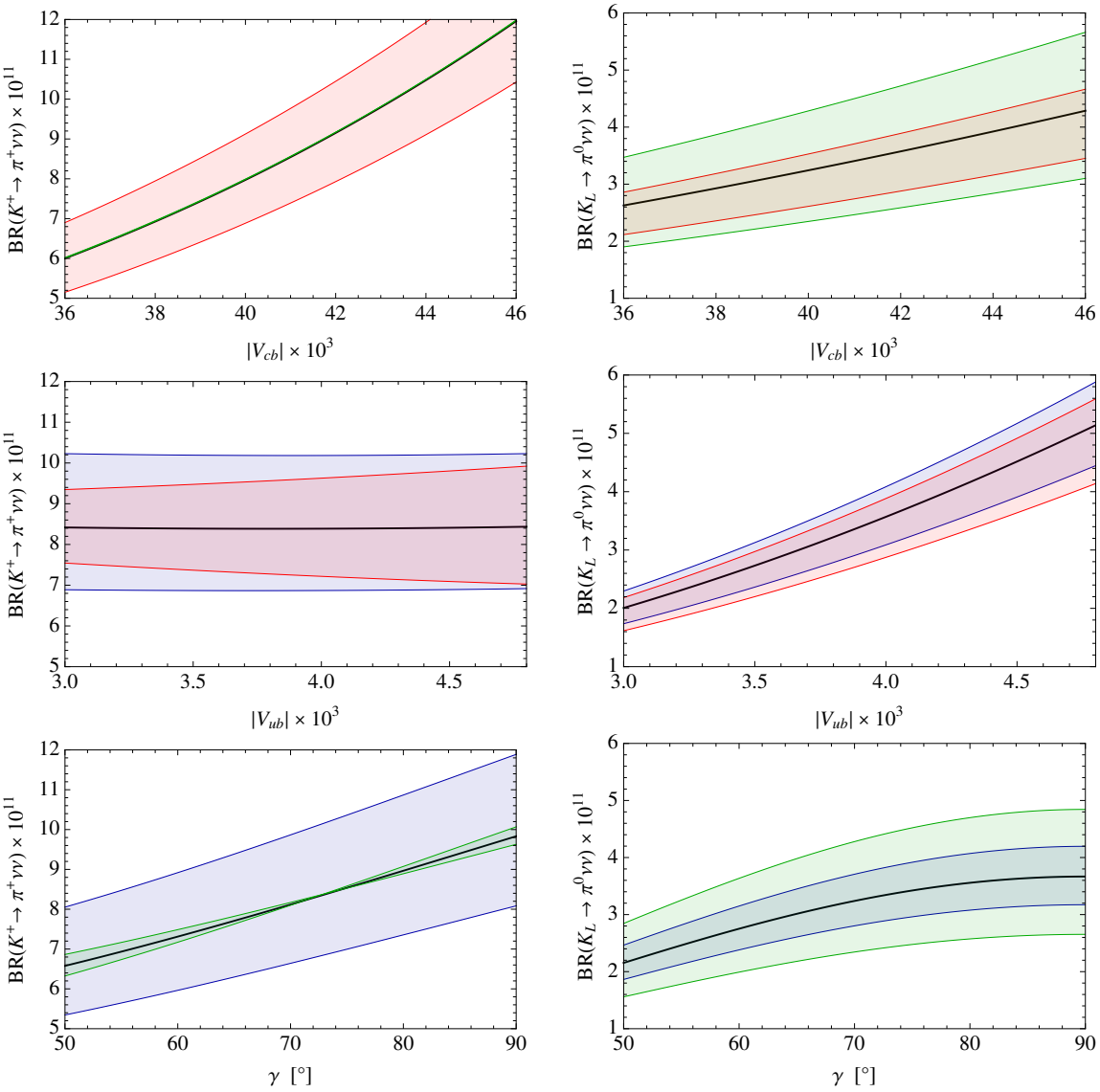

Figure 2. Dependence of the branching ratio observables $\mathcal{B}(K^+ \to \pi^+ \nu\bar{\nu})$ (left) and $\mathcal{B}(K_L \to \pi^0 \nu\bar{\nu})$ (right) on the CKM parameter inputs $|V_{cb}|$, $|V_{ub}|$ and γ. The 95% C.L. bands in V_{ub}, V_{cb} and γ are shown in green, blue, and red, respectively.

Note that both relations are independent of $|V_{cb}|$ and (3.12) depends only on γ. In particular the correlation (3.12) should be of interest in the coming years due to the measurement of $K^+ \to \pi^+ \nu\bar{\nu}$ by NA62, of $B_s \to \mu^+\mu^-$ by LHCb and CMS and of γ by LHCb. Moreover the last factor should also be improved by lattice QCD.

In the left panel of figure 3 we show the correlation between $K^+ \to \pi^+ \nu\bar{\nu}$ and $B_s \to \mu^+\mu^-$ for different fixed values of γ. The dashed regions correspond to a 68% C.L. that results from including the uncertainties on all the other input parameters, whereas the inner filled regions are a result of only including the uncertainties of $|V_{ub}|$, $|V_{cb}|$ (we use the averages in (3.3)), and $|V_{us}|$.

JHEP11(2015)033

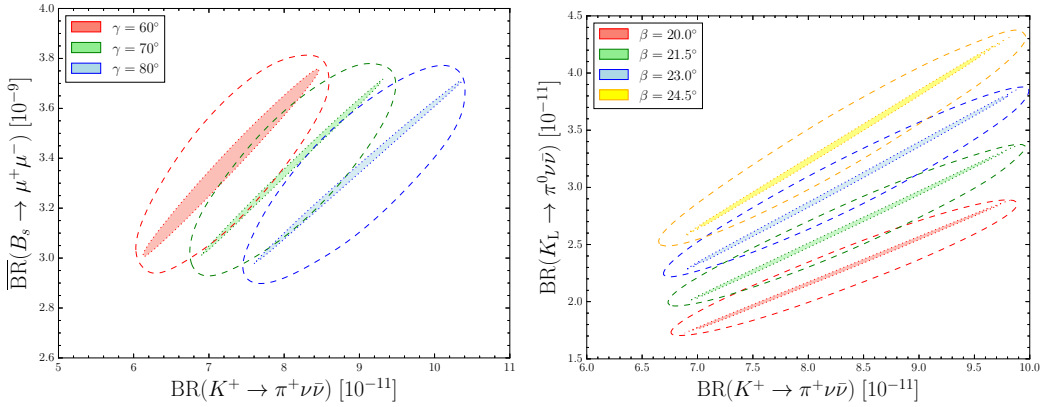

Figure 3. Left panel: correlation of $\overline{\mathcal{B}}(B_s \to \mu^+\mu^-)$ versus $\mathcal{B}(K^+ \to \pi^+\nu\bar{\nu})$ for fixed values of γ. Right panel: correlation of $\mathcal{B}(K_L \to \pi^0\nu\bar{\nu})$ versus $\mathcal{B}(K^+ \to \pi^+\nu\bar{\nu})$ for fixed values of β. In both plots the dashed regions correspond to a 68% C.L. resulting from the uncertainties on all other inputs, while the inner filled regions result from including only the uncertainties from the remaining CKM inputs of strategy A.

It should be noticed that the present experimental determination of $\overline{\mathcal{B}}(B_s \to \mu^+\mu^-)$ is slightly lower than the SM prediction, and the agreement between the SM and the data can be improved by lowering $|V_{cb}|$ to values in the ballpark of its present exclusive determinations. But in this case, as can be seen already from table 1, the SM predictions for both $\mathcal{B}(K^+ \to \pi^+\nu\bar{\nu})$ and ε_K are also reduced. It can be useful to express $\mathcal{B}(K^+ \to \pi^+\nu\bar{\nu})$ as a function of ε_K, in a way similar to (3.12) and (3.13), in order to make the correlation between them explicit. One has

$$\mathcal{B}(K^+ \to \pi^+\nu\bar{\nu}) = (8.39 \pm 1.11) \times 10^{-11} \cdot \left[\frac{|\varepsilon_K|}{2.23 \times 10^{-3}}\right]^{1.07} \times \left[\frac{\gamma}{73.2°}\right]^{-0.11} \cdot \left[\frac{|V_{ub}|}{3.88 \times 10^{-3}}\right]^{-0.95} . \tag{3.14}$$

We do not write explicitly the dependence on the hadronic quantities, since here more parameters are involved. The uncertainty here comes mainly from η_{cc} and η_{ct}, while the ones due to F_K are smaller than the corresponding ones in the $B_{s,d}$ meson systems. It is evident from this formula that a reduction of $\mathcal{B}(K^+ \to \pi^+\nu\bar{\nu})$ implies also a reduction of ε_K.

The correlations in (3.12), (3.13) and (3.14) result from the fact that it is possible, by taking suitable powers of the $B_{s,d} \to \mu^+\mu^-$ branching ratios, to eliminate the dependence on $|V_{cb}|$, while the one-loop functions X, Y, and S are fixed by the top mass in the SM. Both correlations could be broken already in models with constrained MFV (CMFV) in which the modifications of the functions X and Y are generally different. In general MFV models new scalar operators could additionally contribute to $B_{s,d} \to \mu^+\mu^-$, modifying also the factors involving the weak decay constants. Therefore, these correlations are strictly valid only in the SM, and their violation would not necessarily rule out (C)MFV.

$K^+ \to \pi^+\nu\bar{\nu}$ and $K_L \to \pi^0\nu\bar{\nu}$ in Minimal Flavour Violation. In models of NP with Minimal Flavour Violation (MFV) there are no flavour-changing interactions beyond

JHEP11(2015)033

those generated from the SM Yukawa couplings [61]. For $K^+ \to \pi^+\nu\bar{\nu}$ and $K_L \to \pi^0\nu\bar{\nu}$ this restricts the operators that can contribute in most NP models to just the operator already dominant in the SM, $(\bar{s}d)_{V-A}(\bar{\nu}\nu)_{V-A}$, making MFV equivalent to Constrained MFV (CMFV) [62] in this case. Therefore in MFV the value of $X(x_t)$ can be shifted but must stay real. Defining for convenience

$$B_+ = \frac{\mathcal{B}(K^+ \to \pi^+\nu\bar{\nu})}{\kappa_+(1+\Delta_{\rm EM})}, \qquad B_L = \frac{\mathcal{B}(K_L \to \pi^0\nu\bar{\nu})}{\kappa_L}, \tag{3.15}$$

with κ_+ and κ_L given in (2.2) and (2.11), respectively, we have in the case of MFV the correlation

$$B_+ = B_{\rm L} + \left[\frac{{\rm Re}\lambda_t}{{\rm Im}\lambda_t}\sqrt{B_{\rm L}} - \left(1-\frac{\lambda^2}{2}\right){\rm sgn}\left(X(x_t)\right)P_c(X)\right]^2, \tag{3.16}$$

which was first given in [63, 64]. Note that in the SM the sign of $X(x_t)$ is positive. Recalling the relation

$$\frac{{\rm Re}\lambda_t}{{\rm Im}\lambda_t} \simeq -\cot\beta\left(1-\frac{\lambda^2}{2}\right)^2, \tag{3.17}$$

accurate to λ^4 terms, and solving for β then gives

$$\cot\beta = \frac{1}{\left(1-\frac{\lambda^2}{2}\right)^2}\left[\sqrt{\frac{B_+ - B_L}{B_L}} - \left(1-\frac{\lambda^2}{2}\right)\frac{{\rm sgn}\left(X(x_t)\right)P_c(X)}{\sqrt{B_L}}\right]. \tag{3.18}$$

In deriving (3.18) from (3.16) and (3.17) one finds that for $X(x_t) > 0$ this solution is unique, while for $X(x_t) < 0$ a second solution with a minus sign in front of first square root is allowed [64]. However this solution is excluded if we require both branching ratios to be larger than 10^{-11} and we will not consider it here.

In the SM and CMFV we have to a very good approximation the relation [63, 64]

$$S_{\psi K_S} = \sin 2\beta, \tag{3.19}$$

which is only spoiled by possible penguin enhancements in the $B_d \to J/\psi K_{\rm S}$ mode [65]. Thus (3.19) together with (3.18) give a triple correlation between $K^+ \to \pi^+\nu\bar{\nu}$, $K_L \to \pi^0\nu\bar{\nu}$ and $S_{\psi K_S}$ in the SM and CMFV.

As demonstrated in the earlier parts of this section, the branching ratios for $K^+ \to \pi^+\nu\bar{\nu}$ and $K_L \to \pi^0\nu\bar{\nu}$ still contain significant parametric uncertainties due to the uncertainties in $|V_{cb}|$, $|V_{ub}|$ and γ, and to a lesser extent in m_t. It is therefore remarkable that within the SM all these uncertainties practically cancel out in this triple correlation [63]. Moreover, this property turns out to be true for all models with constrained MFV [64].

We note that the main uncertainty in (3.18) resides in P_c, as the uncertainty in λ is very small. We stress that this relation is practically immune to any variation of the function $X(x_t)$ within MFV models. This means that once $\mathcal{B}(K^+ \to \pi^+\nu\bar{\nu})$ and $S_{\psi K_S}$ will be precisely measured we will know the *unique* value of $\mathcal{B}(K_L \to \pi^0\nu\bar{\nu})$ within CMFV models. This relation is analogous to the one between $\mathcal{B}(B_{s,d} \to \mu^+\mu^-)$ and $\Delta M_{s,d}$ [66], where the present knowledge of $\Delta M_{s,d}$ together with the future precise value of $\mathcal{B}(B_s \to \mu^+\mu^-)$ will

JHEP11(2015)033

allow us to uniquely predict the branching ratio $\mathcal{B}(B_d \to \mu^+\mu^-)$ in CMFV models well ahead of its precise direct measurement.

In the right panel of figure 3 we show the correlation between $K^+ \to \pi^+\nu\bar{\nu}$ and $K_L \to \pi^0\nu\bar{\nu}$ for different fixed values of β ($S_{\psi K_S}$). The dashed regions correspond to a 68% C.L. that results from including the uncertainties on all the other input parameters, whereas the inner filled regions are a result of only including the uncertainties of $|V_{cb}|$ (we use the average in (3.3)), γ (as given in (3.4)) and $|V_{us}|$ in (2.7). We observe that in the latter case the dependence on the remaining CKM parameters, for fixed β, is indeed minimal.

It is also possible to express the ratio in (3.17) as

$$\frac{\mathrm{Re}\lambda_t}{\mathrm{Im}\lambda_t} = \frac{\left(1-\frac{\lambda^2}{2}\right)^2}{\sin\gamma}\left[\cos\gamma - \left(\frac{\lambda}{1-\frac{\lambda^2}{2}}\right)\left|\frac{V_{cb}}{V_{ub}}\right|\right], \tag{3.20}$$

i.e. in terms of the tree-level CKM inputs discussed in this section, which are generally assumed to be free of NP effects. We note that in MFV also $S_{\psi K_S}$ is not affected by NP and is more accurately determined than γ. On the other hand, there is a class of models — e.g. models with a $\mathrm{U}(2)^3$ flavour symmetry [67] — where the correlation with $S_{\psi K_S}$ is no longer true, while (3.16) and the generic relation (3.20) still hold.

While the virtue of the correlation (3.18) is its very weak dependence on the CKM parameters, the correlation (3.16) together with (3.20) shares partly this property as it depends only on the ratio $|V_{cb}/V_{ub}|$, equivalent to R_b, and not on $|V_{ub}|$ and $|V_{cb}|$ separately. As we can see from the values of R_b given in table 1, this avoids some of the trouble with exclusive versus inclusive determinations, as the ratio of purely exclusive or inclusive determinations, as well as their weighted average, results in less variation — i.e. only 5% among the cases considered. Note that combining exclusive $|V_{ub}|$ with inclusive $|V_{cb}|$, for example, gives a greater variation.

In the left panel of figure 4 we compare the MFV relation for various values of $|V_{cb}/V_{ub}|$, including a $1\,\sigma$ C.L. region corresponding to our weighted averages. We also include for comparison the relation corresponding to the current $S_{\psi K_S}$ measurement, which is seen to be more accurate. In the right panel we repeat this comparison for possible future constraints in the following decade, where our choice of errors are based on those collected in [19]. For the branching ratios of $K^+ \to \pi^+\nu\bar{\nu}$ and $K_L \to \pi^0\nu\bar{\nu}$ we assume a 10% precision relative to the SM predictions. Though this is the realistic target set by the NA62 experiment for $K^+ \to \pi^+\nu\bar{\nu}$, the KOTO experiment will likely not reach such a precision for $K_L \to \pi^0\nu\bar{\nu}$. We observe that in this possible sketch of the future, the two decays under consideration have the potential to probe MFV and/or a $\mathrm{U}(2)^3$ symmetry.

4 CKM inputs from loop-level observables

A different approach is to assume that there are no relevant NP contributions to all the quantities listed in (1.2), so that we can use them together with the precise value of $|V_{us}|$ to determine the best values of

$$\beta, \qquad |V_{cb}|, \qquad |V_{ub}|, \qquad |V_{td}|, \qquad |V_{ts}|, \tag{4.1}$$

JHEP11(2015)033

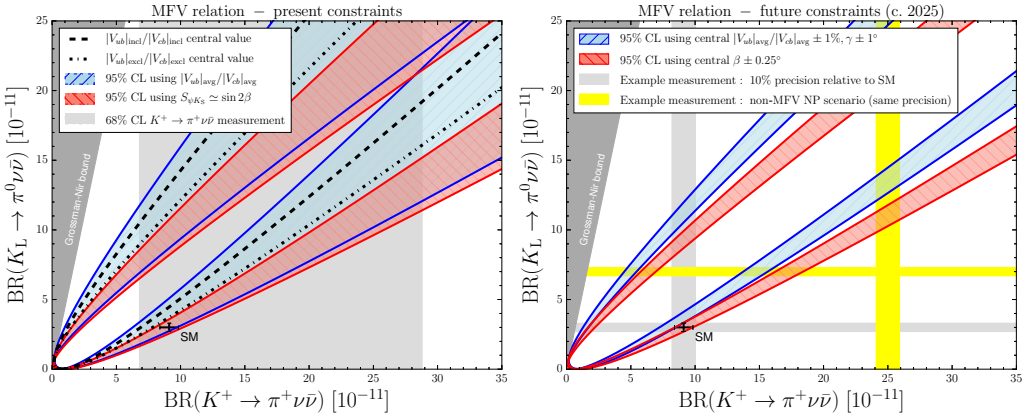

Figure 4. The MFV relation between $K^+ \to \pi^+ \nu\bar{\nu}$ and $K_L \to \pi^0 \nu\bar{\nu}$ using $S_{\psi K_S} \simeq \sin 2\beta$ versus using the various tree-level inputs of $|V_{cb}/V_{ub}|$ and γ (see text). In the left panel we show situation from current constraints, and in the right panel the possible situation in the following decade, including 10% precision on the two branching ratios, for illustration.

and predict the branching ratios for $K^+ \to \pi^+ \nu\bar{\nu}$, $K_L \to \pi^0 \nu\bar{\nu}$ and $B_{s,d} \to \mu^+ \mu^-$. Clearly the absence of NP effects in all the loop observables (1.2) requires the SM to be valid up to a reasonably high energy scale, which is a stronger assumption with respect to the one of strategy A, where only tree-level determinations of CKM parameters were assumed to be free of NP effects. We call this approach strategy B.

The relevant SM expressions can be found in [16] and in particular in [30], where this strategy has been used to determine the correlation between the values of $|V_{cb}|$ and $|V_{ub}|$ with the non-perturbative parameters relevant for $\Delta M_{s,d}$. As the precision on these parameters resulting from QCD lattice calculations is improving, and the value of $\hat{B}_K$, relevant for ε_K, has been known precisely already for some time,[5] we can now use these formulae to extract the values listed in (4.1).

At least three independent observables among the four listed in (1.2) have to be used in order to fix the three free parameters of the CKM matrix besides $|V_{us}|$. For illustration, we present here the strategy which allows us to determine the parameters in (4.1) with high precision with the minimal number of measurements. Schematically this procedure can be described in two steps:

- **Step 1:** the unitarity triangle can be determined from the experimental values of $S_{\psi K_S} = \sin 2\beta$ and the mass ratio

$$\frac{\Delta M_d}{\Delta M_s} = \frac{m_{B_d}}{m_{B_s}} \frac{1}{\xi^2} \frac{|V_{td}|^2}{|V_{ts}|^2}, \qquad \xi \equiv \frac{F_{B_s}\sqrt{\hat{B}_{B_s}}}{F_{B_d}\sqrt{\hat{B}_{B_d}}}. \tag{4.2}$$

[5] We use $\hat{B}_K = 0.750(15)$ which takes into account the values obtained by lattice QCD [44] and large N approach [46].

JHEP11(2015)033

Using the following very accurate expressions for $|V_{td}|$ and $|V_{ts}|$,

$$|V_{td}| \simeq \lambda |V_{cb}| R_t, \qquad |V_{ts}| \simeq \left(1 + \frac{\lambda^2}{2}(1 - 2R_t \cos\beta)\right) |V_{cb}|, \tag{4.3}$$

where R_t is one of the sides of the UT, and solving (4.2) for R_t one gets

$$R_t \simeq \frac{\xi}{|V_{us}|} \sqrt{\frac{\Delta M_d}{\Delta M_s} \frac{m_{B_s}}{m_{B_d}}} \left(1 - |V_{us}| \xi \sqrt{\frac{\Delta M_d}{\Delta M_s} \frac{m_{B_s}}{m_{B_d}}} + \frac{|V_{us}|^2}{2} + \cdots\right) \tag{4.4}$$

where the dots indicate terms of order $\mathcal{O}(|V_{us}|^4, |V_{us}|^2 \Delta M_d / \Delta M_s)$.

With one side, R_t, and one angle, β, known, the full unitarity triangle is determined by means of purely geometrical relations. In particular one has

$$R_b = \frac{1 - \lambda^2/2}{\lambda} \left|\frac{V_{ub}}{V_{cb}}\right| = \sqrt{1 + R_t^2 - 2R_t \cos\beta}, \qquad \cot\gamma = \frac{1 - R_t \cos\beta}{R_t \sin\beta}, \tag{4.5}$$

and the apex $(\bar{\varrho}, \bar{\eta})$ of the triangle is given by

$$\bar{\varrho} = 1 - R_t \cos\beta, \qquad \bar{\eta} = R_t \sin\beta\,. \tag{4.6}$$

The very precise value of R_t obtained through $\Delta M_d / \Delta M_s$ therefore allows a very precise determination of γ.

It should be emphasised that the UT constructed in this manner is universal for all CMFV models as the box function S does not enter the expressions used in these two steps [62]. Moreover this determination is independent of $|V_{cb}|$.

- **Step 2:** the measured value of $|\varepsilon_K|$ then allows us to determine the optimal value of $|V_{cb}|$. Indeed we have [68]

$$\begin{aligned} |\varepsilon_K^{\rm SM}| = {} & \kappa_\varepsilon \frac{G_F^2 F_K^2 m_{K^0} M_W^2}{6\sqrt{2}\pi^2 \Delta M_K} \hat{B}_K |V_{cb}|^2 \lambda^2 R_t \sin\beta, \\ & \times \left(|V_{cb}|^2 R_t \cos\beta\, \eta_{tt} S_0(x_t) + \eta_{ct} S_0(x_c, x_t) - \eta_{cc} x_c\right) \end{aligned} \tag{4.7}$$

where $x_i = m_i^2 / M_W^2$, S_0 is the well known SM box function as defined e.g. in [16], and $\kappa_\varepsilon = 0.94 \pm 0.02$ [68, 69]. With R_t known from (4.3) and β determined from $S_{\psi K_S}$, the only unknown in (4.7) is $|V_{cb}|$. Having found $|V_{cb}|$, R_b, and R_t, also $|V_{ub}|$, $|V_{td}|$ and $|V_{ts}|$ are determined by the previous relations in a straightforward way.

Alternatively we can also determine $|V_{cb}|$ by using separately $\Delta M_s \propto |V_{ts}|^2$ and $\Delta M_d \propto |V_{td}|^2$ instead of ϵ_K, as both are proportional to $|V_{cb}|^2$ via the expressions given in (4.4). In principle it is also possible to determine the CKM matrix from ΔM_d, ΔM_s, and ϵ_K, but the precision in this case will be rather limited, due to the absence of the strong constraint on β from $S_{\psi K_S}$. The best accuracy is obtained by performing a simultaneous fit to all the four observables ΔM_d, ΔM_s, $S_{\psi K_S}$ and ϵ_K.

In table 3 we give the results of fits for the CKM matrix elements using different combinations of the inputs discussed in the steps above. The values for the experimental

JHEP11(2015)033

	$\{\lvert\varepsilon_K\rvert, \Delta M_d/\Delta M_s, S_{\psi K_S}\}_{\rm SM}$	$\{\Delta M_d, \Delta M_s, S_{\psi K_S}\}_{\rm SM}$	$\{\lvert\varepsilon_K\rvert, \Delta M_d, \Delta M_s, S_{\psi K_S}\}_{\rm SM}$
$\lvert V_{cb}\rvert$ $[10^{-3}]$	$42.59^{+1.41}_{-1.26}$	$41.30^{+2.65}_{-2.47}$	$42.35^{+1.25}_{-1.13}$
$\lvert V_{ub}\rvert$ $[10^{-3}]$	$3.62^{+0.15}_{-0.14}$	$3.51^{+0.27}_{-0.25}$	$3.61^{+0.15}_{-0.14}$
$\lvert V_{td}\rvert$ $[10^{-3}]$	$8.96^{+0.28}_{-0.28}$	$8.68^{+0.66}_{-0.62}$	$8.95^{+0.27}_{-0.28}$
$\lvert V_{ts}\rvert$ $[10^{-3}]$	$41.79^{+1.43}_{-1.27}$	$40.52^{+2.60}_{-2.42}$	$41.55^{+1.27}_{-1.14}$
$\mathcal{B}(K^+ \to \pi^+\nu\bar{\nu})$ $[10^{-11}]$	$9.18^{+0.79}_{-0.71}$	$8.39^{+1.76}_{-1.41}$	$9.08^{+0.74}_{-0.68}$
$\mathcal{B}(K_L \to \pi^0\nu\bar{\nu})$ $[10^{-11}]$	$3.01^{+0.33}_{-0.29}$	$2.66^{+0.84}_{-0.63}$	$2.98^{+0.32}_{-0.28}$
$\overline{\mathcal{B}}(B_s \to \mu^+\mu^-)$ $[10^{-9}]$	$3.69^{+0.30}_{-0.26}$	$3.46^{+0.49}_{-0.43}$	$3.64^{+0.27}_{-0.24}$
$\mathcal{B}(B_d \to \mu^+\mu^-)$ $[10^{-10}]$	$1.09^{+0.08}_{-0.08}$	$1.02^{+0.17}_{-0.15}$	$1.09^{+0.08}_{-0.08}$
$\mathrm{Im}(\lambda_t)$ $[10^{-4}]$	$1.43^{+0.08}_{-0.07}$	$1.35^{+0.20}_{-0.17}$	$1.42^{+0.07}_{-0.07}$
$\mathrm{Re}(\lambda_t)$ $[10^{-4}]$	$-3.46^{+0.18}_{-0.19}$	$-3.25^{+0.40}_{-0.45}$	$-3.43^{+0.17}_{-0.18}$

Table 3. Results of the fit to the CKM matrix elements for various combinations of inputs as detailed in strategy B, and the corresponding observable predictions.

and lattice observables used as inputs are listed in table 2. The fits were performed using a Bayesian statistical approach: uncorrelated Gaussian priors were chosen for each of the input parameters and the posterior distribution was sampled using Markov Chain Monte Carlo with the help of the Bayesian Analysis Toolkit [70]. A direct minimisation of the χ^2, yielding identical results, has also been performed as a check. We observe that using $|\varepsilon_K|$ in step 2 gives a more precise result for $|V_{cb}|$ than the alternative of using ΔM_d and ΔM_d separately, as well as favouring a higher central value. The most accurate determination (given in the last column of the table), follows from including all inputs. The corresponding CKM matrix elements of interest are:

$$|V_{ub}| = (3.61 \pm 0.14) \times 10^{-3}, \qquad |V_{cb}| = (42.4 \pm 1.2) \times 10^{-3},$$
$$|V_{td}| = (8.94 \pm 0.27) \times 10^{-3}, \qquad |V_{ts}| = (41.6 \pm 1.2) \times 10^{-3}. \tag{4.8}$$

For completeness, we give here the sides of the UT as determined from our full fit, that read

$$R_t = 0.937 \pm 0.032, \qquad R_b = 0.368 \pm 0.013, \tag{4.9}$$

while its angles are

$$\alpha = (89.0 \pm 5.0)^\circ, \qquad \beta = (21.5 \pm 0.8)^\circ, \qquad \gamma = (69.5 \pm 5.0)^\circ, \tag{4.10}$$

and its apex

$$\bar{\varrho} = 0.129 \pm 0.030, \qquad \bar{\eta} = 0.344 \pm 0.017. \tag{4.11}$$

The precision on R_t, γ and $|V_{cb}|$ using the above strategy is already impressive, and will continue to improve with new lattice results. Using for instance the improved error

JHEP11(2015)033

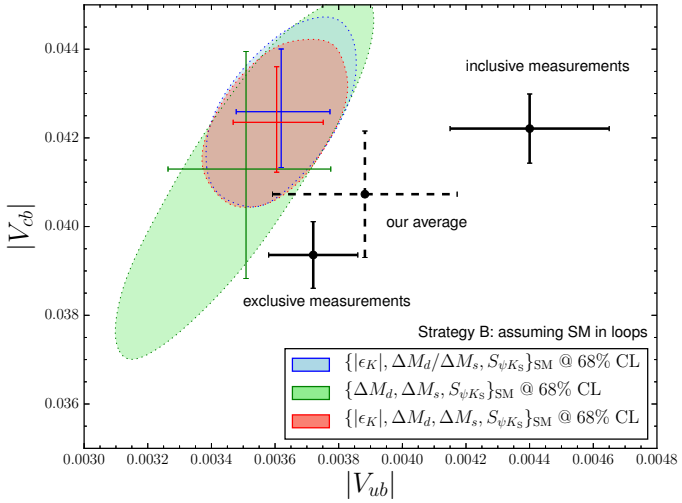

Figure 5. Comparison of 68% C.L. regions for $|V_{ub}|$ and $|V_{cb}|$ in strategy B for various combinations of inputs versus their reported inclusive and exclusive values, and our averages of these, as considered in strategy A.

estimates for ξ and $f_{B_s}\sqrt{\hat{B}_{B_s}}$ from [31] (keeping the central values from [44]) we find the very precise results:

$$|V_{cb}| = (42.0 \pm 0.9) \times 10^{-3}, \qquad \gamma = (70.8 \pm 2.3)^\circ, \qquad R_t = 0.945 \pm 0.015. \tag{4.12}$$

In figure 5 we show the fitted ranges for $|V_{ub}|$ and $|V_{cb}|$ and compare them with the inclusive, exclusive and our averaged values in (3.1)–(3.3). We distinguish between three different cases: the blue area corresponds to the fitted range of $|V_{ub}|$ and $|V_{cb}|$ determined by $|\varepsilon_K|$, $\Delta M_d/\Delta M_s$ and $S_{\psi K_S}$; for the green area ΔM_d, ΔM_s and $S_{\psi K_S}$ are used as inputs and the red area combines both and uses $|\varepsilon_K|$, ΔM_d, ΔM_s and $S_{\psi K_S}$ as inputs. As noted earlier, one can see that especially $|\varepsilon_K|$ favours large values of $|V_{cb}|$, around the inclusive value, while the rather small $|V_{ub}|$, around the exclusive value, is favoured by $S_{\psi K_S}$.

It is interesting to compare these results with the indirect fits performed by UTfit [27] and CKMfitter [28], which give

$$\text{UTfit:} \quad |V_{ub}| = (3.63 \pm 0.12) \times 10^{-3}, \qquad |V_{cb}| = (41.7 \pm 0.56) \times 10^{-3}, \tag{4.13}$$

$$\text{CKMfitter:} \quad |V_{ub}| = \left(3.55^{+0.17}_{-0.15}\right) \times 10^{-3}, \qquad |V_{cb}| = \left(41.17^{+0.90}_{-1.14}\right) \times 10^{-3}. \tag{4.14}$$

They are in very good agreement with our results. We note however, that these two groups included in their analyses the information from tree level decays, which we have decided not to include in our strategy B because of the discrepancies between inclusive and exclusive determinations of $|V_{ub}|$ and $|V_{cb}|$. Moreover, we also did not use the tree-level determination of γ contrary to these two groups.

Having determined the full CKM matrix in this manner, predictions for rare decays branching ratios can be made. These are collected in the last four rows in table 3 and again the most precise are the ones in the last column so that our final results for the four

JHEP11(2015)033

branching ratios are:

$$\mathcal{B}(K^+ \to \pi^+ \nu\bar{\nu}) = (9.11 \pm 0.72) \times 10^{-11}, \tag{4.15}$$
$$\mathcal{B}(K_L \to \pi^0 \nu\bar{\nu}) = (3.00 \pm 0.31) \times 10^{-11}, \tag{4.16}$$
$$\overline{\mathcal{B}}(B_s \to \mu^+ \mu^-) = (3.66 \pm 0.26) \times 10^{-9}, \tag{4.17}$$
$$\mathcal{B}(B_d \to \mu^+ \mu^-) = (1.09 \pm 0.08) \times 10^{-10}. \tag{4.18}$$

In (4.12) we used the new lattice error estimates from [31] for a "sneak preview" of how the CKM fit in strategy B will improve once the full results will be available. Using these results for the observable predictions listed above will likewise lead to reduced uncertainties: $\delta\mathcal{B}(K^+ \to \pi^+ \nu\bar{\nu}) = 0.65$, $\delta\mathcal{B}(K_L \to \pi^0 \nu\bar{\nu}) = 0.28$, $\delta\mathcal{B}(B_s \to \mu^+ \mu^-) = 0.22$ and $\delta\mathcal{B}(B_d \to \mu^+ \mu^-) = 0.07$.

As a comparison, using instead the fit results of (4.13) and (4.14), one gets

$$\text{UTfit:} \quad \mathcal{B}(K^+ \to \pi^+ \nu\bar{\nu}) = \left(8.64^{+0.54}_{-0.53}\right) \times 10^{-11}, \tag{4.19}$$
$$\mathcal{B}(K_L \to \pi^0 \nu\bar{\nu}) = (2.93 \pm 0.25) \times 10^{-11}, \tag{4.20}$$
$$\text{CKMfitter:} \quad \mathcal{B}(K^+ \to \pi^+ \nu\bar{\nu}) = \left(8.17^{+0.61}_{-0.71}\right) \times 10^{-11}, \tag{4.21}$$
$$\mathcal{B}(K_L \to \pi^0 \nu\bar{\nu}) = \left(2.65^{+0.29}_{-0.28}\right) \times 10^{-11}. \tag{4.22}$$

It is also interesting to compare the results in (4.17), (4.18) with the most recent prediction in the SM [71], with which our SM results are in perfect agreement,[6] and with the most recent averages from the combined analysis of CMS and LHCb [72] that read

$$\overline{\mathcal{B}}(B_s \to \mu^+ \mu^-) = (2.8^{+0.7}_{-0.6}) \times 10^{-9}, \tag{4.23}$$
$$\mathcal{B}(B_d \to \mu^+ \mu^-) = (3.9^{+1.6}_{-1.4}) \times 10^{-10}. \tag{4.24}$$

Note that the SM value of $\overline{\mathcal{B}}(B_s \to \mu^+ \mu^-)$ is outside one sigma range of the experimental value.

In figure 6 the correlations of $\mathcal{B}(K_L \to \pi^0 \nu\bar{\nu})$ and $\overline{\mathcal{B}}(B_s \to \mu^+ \mu^-)$ versus $\mathcal{B}(K^+ \to \pi^+ \nu\bar{\nu})$ are shown, comparing the best result of strategy B, which includes all of the available inputs, with the inclusive, exclusive and average cases of strategy A. We observe that the inclusive case of strategy A is very similar to strategy B for $K^+ \to \pi^+ \nu\bar{\nu}$ and $B_s \to \mu^+ \mu^-$, as both have little sensitivity to $|V_{ub}|$, whereas $K_L \to \pi^0 \nu\bar{\nu}$, which has a stronger $|V_{ub}|$ dependence, can differentiate them. In both plots our average for $|V_{ub}|$ and $|V_{cb}|$ is seen to also pick the middle ground for these observables.

Evidently, the present experimental value for $\overline{\mathcal{B}}(B_s \to \mu^+ \mu^-)$ in (4.23) would favour the exclusive determination of $|V_{cb}|$ and a value of $\mathcal{B}(K^+ \to \pi^+ \nu\bar{\nu})$ in the ballpark of 7×10^{-11} rather than 9×10^{-11}. But then also the value of $|\varepsilon_K|$ would be below the data. It appears then that unless the experimental value for $\overline{\mathcal{B}}(B_s \to \mu^+ \mu^-)$ moves up by 20% in the coming years, the SM will face some tensions in this sector of flavour physics.

[6] This is not surprising as these authors used the inclusive determination of $|V_{cb}|$ that is very close to the value determined by us.

JHEP11(2015)033

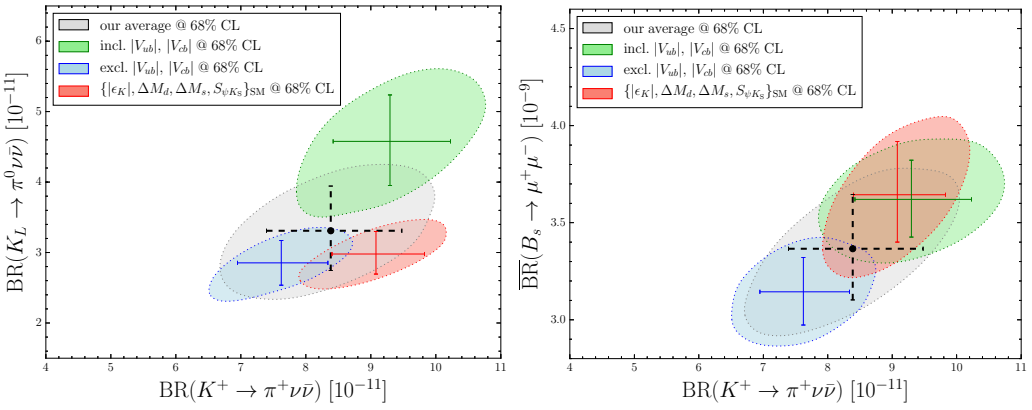

Figure 6. Comparison of 68% C.L. regions for $\mathcal{B}(K_L \to \pi^0\nu\bar{\nu})$ and $\overline{\mathcal{B}}(B_s \to \mu^+\mu^-)$ versus $\mathcal{B}(K^+ \to \pi^+\nu\bar{\nu})$, using different inputs from both strategy A and B to fix the CKM matrix .

It is instructive to recall the following formula [3, 73] that summarises the dependence of $\mathcal{B}(K^+ \to \pi^+\nu\bar{\nu})$ on R_t, β and V_{cb}:

$$\mathcal{B}(K^+ \to \pi^+\nu\bar{\nu}) = \frac{\kappa_+}{\lambda^8}\,|V_{cb}|^4 X(x_t)^2 \left[\frac{R_t^2 \sin^2\beta}{(1-\lambda^2/2)^2} + \left(1-\frac{\lambda^2}{2}\right)^2 \left(R_t\cos\beta + \frac{\lambda^4 P_c(X)}{|V_{cb}|^2 X(x_t)}\right)^2\right]. \quad (4.25)$$

This can be considered as the fundamental formula for a correlation between $\mathcal{B}(K^+ \to \pi^+\nu\bar{\nu})$, β and any observable used to determine R_t, and is valid also in all models with MFV where $X(x_t)$ is replaced by a real function X. When this formula was proposed, it contained significant uncertainties in R_t determined through $\Delta M_d/\Delta M_s$, in $P_c(X)$ known only at NLO, in κ_+ and in $|V_{cb}|$. The first three uncertainties have been significantly reduced since then. Moreover, the improved knowledge of the non-perturbative parameters entering ε_K and $\Delta M_{s,d}$ allows now within the SM to determine $|V_{cb}|$ rather precisely. We stress that in other models with MFV the latter determination will depend on the NP contributions to ε_K and $\Delta M_{s,d}$ which modify the function S. An analysis of this issue is presented in [30].

Finally when γ from tree-level decays will be precisely measured, R_t will be determined solely by β and γ,

$$R_t = \frac{\sin\gamma}{\sin(\beta+\gamma)}, \quad (4.26)$$

and the dependence of $\mathcal{B}(K^+ \to \pi^+\nu\bar{\nu})$ on γ can be directly read off (4.25).

5 The ratio ε'/ε in the Standard Model

The ratio ε'/ε measures the size of direct CP violation in $K_L \to \pi\pi$ relative to the indirect CP violation described by ε_K. In the SM ε' is governed by QCD penguins, but receives also an important destructively interfering contribution from electroweak penguins that is generally much more sensitive to NP than the QCD contribution.

JHEP11(2015)033

The ratio ε'/ε is measured to be [38, 74–76]

$$\mathrm{Re}(\varepsilon'/\varepsilon) = (16.5 \pm 2.6) \times 10^{-4}, \tag{5.1}$$

and the imaginary part of ε'/ε is negligible so that we will just write ε'/ε in all formulae below.

This result constitutes in principle a strong constraint on theory. However, the difficulty in making predictions for ε'/ε within the SM and its extensions is the strong cancellation of QCD penguin contributions and electroweak penguin contributions to this ratio. In the SM QCD penguins give a positive contribution, while the electroweak penguins a negative one. In order to obtain a useful prediction for ε'/ε in the SM the corresponding hadronic parameters $B_6^{(1/2)}$ and $B_8^{(3/2)}$ have to be known precisely.

In the large N limit one has $B_6^{(1/2)} = B_8^{(3/2)} = 1$ [77–79]. While the study of $1/N$ corrections in [80] indicated that $B_8^{(3/2)} < 1$, no conclusive result has been obtained for $B_6^{(1/2)}$. Fortunately, very recently significant progress on both $B_6^{(1/2)}$ and $B_8^{(3/2)}$ has been made by lattice QCD simulations and in the context of the large N approach. Indeed, from the results of the RBC-UKQCD collaboration [81, 82] one can extract

$$B_6^{(1/2)} = 0.57 \pm 0.19, \qquad B_8^{(3/2)} = 0.76 \pm 0.05\,, \qquad \text{(lattice QCD)} \tag{5.2}$$

as shown in appendix C in the case of $B_8^{(3/2)}$, and in [83, 84] for $B_6^{(1/2)}$. On the other hand, the very recent analysis in the large-N approach in [84] allows to derive a conservative upper bound on both $B_6^{(1/2)}$ and $B_8^{(3/2)}$, which reads

$$B_6^{(1/2)} \le B_8^{(3/2)} < 1. \qquad \text{(large-}N\text{)} \tag{5.3}$$

Moreover, one finds $B_8^{(3/2)}(m_c) = 0.80 \pm 0.10$ in good agreement with (5.2). The result for $B_6^{(1/2)}$ is less precise but there is a strong indication that $B_6^{(1/2)} < B_8^{(3/2)}$, also in agreement with (5.2). We refer to [84] for further arguments why $B_6^{(1/2)}$ is expected to be smaller than $B_8^{(3/2)}$.

The most recent analysis of ε'/ε has been given in [83]. Using the results in (5.2) and determining the remaining contributions to ε'/ε by imposing the agreement of the SM with CP-conserving data one finds[7] [83]

$$\mathrm{Re}(\varepsilon'/\varepsilon) = (1.9 \pm 4.5) \times 10^{-4}\,, \tag{5.4}$$

significantly below the experimental value in (5.1). This result differs by roughly 3σ from the data, but, as stressed in [83], larger values can be obtained if only the absolute large N upper bound on both parameters in (5.3) is used. Yet, as found there and confirmed here by us, even with more generous values of $\mathrm{Im}\lambda_t$ the SM has serious difficulty in describing the data for ε'/ε.

In spite of this it is of interest to study the correlation of ε'/ε with $K_L \to \pi^0\nu\bar{\nu}$ in the SM as this correlation has been already studied in various extensions of the SM [23, 85–90].

[7] To this end $\mathrm{Im}\,\lambda_t = (1.4 \pm 0.1) \times 10^{-4}$ has been used.

JHEP11(2015)033

Within the SM this correlation depends only on the values of $B_6^{(1/2)}$ and $B_8^{(3/2)}$ and the CKM parameters which we determined in the previous sections using strategies A and B.

All the relevant details on ε'/ε within the SM including the relevant references are given in [83]. Here we collect only the relevant information necessary to perform the numerical analysis. The basic analytic formula for ε'/ε reads [83]

$$\left(\frac{\varepsilon'}{\varepsilon}\right)_{\rm SM} = {\rm Im}\lambda_t \cdot F_{\varepsilon'}(x_t), \tag{5.5}$$

where

$$F_{\varepsilon'}(x_t) = P_0 + P_X\, X_0(x_t) + P_Y\, Y_0(x_t) + P_Z\, Z_0(x_t) + P_E\, E_0(x_t)\,, \tag{5.6}$$

with the first term dominated by QCD-penguin contributions, the next three terms by electroweak penguin contributions, and the last term being totally negligible. The x_t dependent functions have been collected in appendix C.

The coefficients P_i are given in terms of the non-perturbative parameters R_6 and R_8 defined in (5.8) as follows:

$$P_i = r_i^{(0)} + r_i^{(6)} R_6 + r_i^{(8)} R_8\,. \tag{5.7}$$

The coefficients $r_i^{(0)}$, $r_i^{(6)}$ and $r_i^{(8)}$ comprise information on the Wilson-coefficient functions of the $\Delta S = 1$ weak effective Hamiltonian at NLO. Their numerical values are given in the NDR renormalisation scheme for $\mu = m_c$ and three values of $\alpha_s(M_Z)$ in table 4 in appendix C.

The parameters R_6 and R_8 are directly related to the parameters $B_6^{(1/2)}$ and $B_8^{(3/2)}$ representing the hadronic matrix elements of Q_6 and Q_8, respectively. They are defined as

$$R_6 \equiv B_6^{(1/2)} \left[\frac{114.54\,{\rm MeV}}{m_s(m_c)+m_d(m_c)}\right]^2, \tag{5.8}$$

$$R_8 \equiv B_8^{(3/2)} \left[\frac{114.54\,{\rm MeV}}{m_s(m_c)+m_d(m_c)}\right]^2. \tag{5.9}$$

We stress that both $B_6^{(1/2)}$ and $B_8^{(3/2)}$ depend very weakly on the renormalisation scale [91].

In figure 7 we show the correlation between ε'/ε and $K_L \to \pi^0\nu\bar{\nu}$ in the SM. The central value from the RBC-UKQCD collaboration in (5.2) has been used for $B_8^{(3/2)}$. The different colours correspond to different choices of the parameter $B_6^{(1/2)}$:

$$B_6^{(1/2)} = 1.0 \qquad \text{(blue)}, \tag{5.10}$$

$$B_6^{(1/2)} = 0.76 \qquad \text{(green)}, \tag{5.11}$$

$$B_6^{(1/2)} = 0.57 \qquad \text{(red)}\,. \tag{5.12}$$

The first choice is motivated by the upper limit from large N approach in (5.3), although the bound $B_6^{(1/2)} < B_8^{(3/2)}$ is violated, and gives an idea of the largest possible values of ε'/ε attainable in the SM. The second choice assumes that $B_6^{(1/2)} = B_8^{(3/2)}$ is saturating the previous bound. Finally, the third choice uses the central values (5.2) from the RBC-UKQCD collaboration for both $B_6^{(1/2)}$ and $B_8^{(3/2)}$. We observe that even for the first choice

JHEP11(2015)033

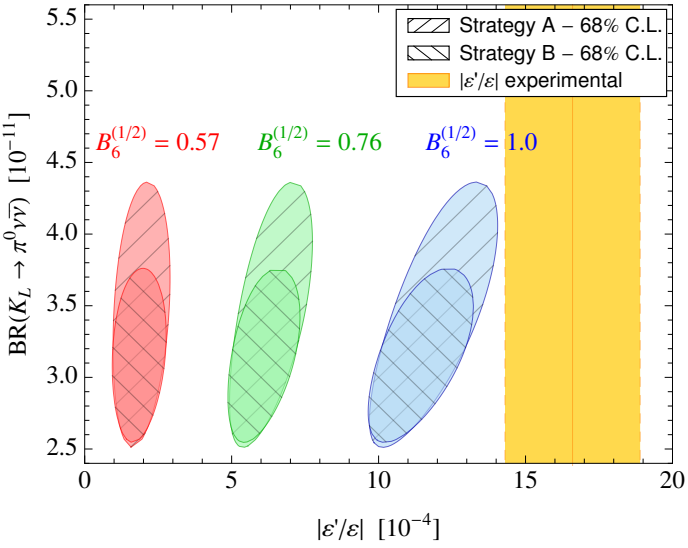

Figure 7. Correlation of $\mathcal{B}(K_L \to \pi^0\nu\bar{\nu})$ versus $|\varepsilon'/\varepsilon|$ for fixed values of $B_6^{(1/2)} = 0.57$ (red), 0.76 (green), and 1.00 (blue). The hatched regions correspond to a 68% C.L. resulting from the uncertainties on all other inputs, for strategy A using our average values of $|V_{ub}|$ and $|V_{cb}|$, and strategy B. The yellow band shows the experimental result at 1σ.

of $B_6^{(1/2)}$ and $B_8^{(3/2)}$ the ratio ε'/ε in the SM is below the data, and only for the largest values of $\mathrm{Im}\lambda_t$ it is within 2σ from the central experimental value. For such values also the branching ratio for $K_L \to \pi^0\nu\bar{\nu}$ is largest.

6 Summary and outlook

In this paper we have performed a new analysis of the rare decays $K^+ \to \pi^+\nu\bar{\nu}$ and $K_L \to \pi^0\nu\bar{\nu}$ within the SM. The prime motivations for this study were:

- The start of the NA62 experiment that should in the coming years reach a precision of 10% relative to the SM prediction for $\mathcal{B}(K^+ \to \pi^+\nu\bar{\nu})$.

- The soon to improve value of ξ, for which preliminary error estimates are already given in [31], which will allow a much more precise determination of the elements of the CKM matrix, in particular of the angle γ, $|V_{ub}|$ and $|V_{cb}|$, without the use of present tree-level determinations of these parameters that are presently subject to significant uncertainties.

- The observation of the correlation between $\mathcal{B}(K^+ \to \pi^+\nu\bar{\nu})$, $\mathcal{B}(B_s \to \mu^+\mu^-)$ and γ within the SM that only weakly depends on $|V_{cb}|$. This correlation should be of interest in particular for CERN experimentalists who in the coming years will significantly improve the measurements on these three quantities.

Our main results are illustrated with several plots in sections 3 and 4. Our analysis demonstrates that in the coming years the SM will undergo an unprecedented test due to

JHEP11(2015)033

the measurements of the rates for the decays $K^+ \to \pi^+\nu\bar{\nu}$ and $B_s \to \mu^+\mu^-$ and improved determinations of the CKM parameters either through the strategies A or B, accompanied by improved lattice QCD calculations of the relevant non-perturbative parameters. Around 2020 these studies will be enriched through precise measurements of the rates for $K_L \to \pi^0\nu\bar{\nu}$, $B_d \to \mu^+\mu^-$ and $B_d \to K(K^*)\nu\bar{\nu}$ [92].

Also improved knowledge of the parameters $B_6^{(1/2)}$ and $B_8^{(3/2)}$, accompanied with improved values of CKM parameters, will allow a more precise prediction for the important ratio ε'/ε. Calculating this ratio using strategies A and B we find, in accordance with the recent analysis in [83], that the SM prediction for ε'/ε is significantly below the data leaving large room for NP contributions. A recent analysis of ε'/ε in simplified NP models has shown which NP models could move the theory prediction for ε'/ε to agree with data [89]. Needless to say, in order to be sure that the SM indeed fails in the description of data, a big effort in clarifying various uncertainties will be required, as discussed in [83].

It should be observed that the agreement of the SM prediction for $\overline{\mathcal{B}}(B_s \to \mu^+\mu^-)$ with the data can be significantly improved by lowering $|V_{cb}|$ to the values in the ballpark of its present exclusive determinations using lattice QCD form factors. But then automatically ε_K is found significantly below the data. Interestingly in this case $\mathcal{B}(K^+ \to \pi^+\nu\bar{\nu})$ is also predicted to be in the ballpark of 7×10^{-11}, that is more than a factor of two below its present experimental average. No doubt, the coming years will be exceptional for quark flavour physics.

Acknowledgments

We thank Aida X. El-Khadra and Andreas S. Kronfeld for illuminating and informative discussions about their lattice calculations of $\Delta B = 2$ matrix elements and Tadeusz Jankowski and Chris Sachrajda for the insight in their calculation of $\Delta I = 3/2$ $K \to \pi\pi$ matrix elements. This research was done and financed in the context of the ERC Advanced Grant project "FLAVOUR"(267104) and was partially supported by the DFG cluster of excellence "Origin and Structure of the Universe".

A Expression for X_t

The loop function X_t of (2.4) can be written as

$$X(x_t) = X_0(x_t) + \frac{\alpha_s}{4\pi} X_1(x_t) + \frac{\alpha}{4\pi} X_{\rm EW}(x_t), \tag{A.1}$$

where X_0 is the leading order result, and X_1, $X_{\rm EW}$ are the NLO QCD and EW corrections, respectively. The coupling constants α_s and α, as well as the parameter $x_t = m_t^2/m_W^2 = 2y_t^2/g_2^2$, have to be evaluated at a given renormalisation scale $\mu \sim \mathcal{O}(M_t)$.

The LO expression is

$$X_0(x_t) = \frac{x_t}{8}\left[\frac{x_t+2}{x_t-1} + \frac{3x_t-6}{(x_t-1)^2}\log x_t\right]. \tag{A.2}$$

The NLO QCD correction [1–3] reads, in the $\overline{\text{MS}}$ scheme,

$$\begin{aligned} X_1(x_t) = &- \frac{29x_t - x_t^2 - 4x_t^3}{3(1-x_t)^2} - \frac{x_t + 9x_t^2 - x_t^3 - x_t^4}{(1-x_t)^3} \log x_t \\ &+ \frac{8x_t + 4x_t^2 + x_t^3 - x_t^4}{2(1-x_t)^3} \log^2 x_t - \frac{4x_t - x_t^3}{(1-x_t)^2} \text{Li}_2(1-x_t) \\ &+ 8x_t \frac{\partial X_0}{\partial x_t} \log \frac{\mu^2}{M_W^2}, \end{aligned} \tag{A.3}$$

where μ is the renormalisation scale. The 2-loop EW correction X_{EW} has been calculated in [8], but no explicit result has been presented. Approximate formulae, one of which accurate to more than 0.05%, as well as a plot of the contribution $(\alpha/4\pi)X_{\text{EW}}$ can however be found in [8].

The left panel of figure 8 shows a plot of the scale- and scheme-independent quantity

$$\tilde{X}(\mu) = \frac{\alpha(\mu)}{\sin^2\theta_w(\mu)} \frac{\sin^2\theta_w(M_Z)}{\alpha(M_Z)} X(x_t(\mu), \mu) \tag{A.4}$$

as a function of the renormalisation scale μ, together with the 1σ bands corresponding to the theoretical error in the matching of the top Yukawa coupling y_t at the weak scale, and the experimental error on the top mass M_t. The $\overline{\text{MS}}$ couplings at full NNLO — 2-loop matching at the weak scale (3-loop QCD for α_s and y_t) and 3-loop running (4-loop QCD for α_s) — as determined in [34] have been used. The remaining scale dependence shown in the figure comes from higher order corrections, mainly from QCD, and accounts for an error of 0.004 on X_t. An additional error of 0.002 comes from the ambiguity in the choice of the renormalisation scheme for the EW prefactor, as shown in [8]. A comparison of the different errors contributing to X_t is shown in the right panel of figure 8. The experimental error on the top quark pole mass M_t is by far the dominant contribution at present.

B Expression for $P_c(X)$

An approximate formula for $P_c^{\text{SD}}(X)$ taken from [7] reads

$$\begin{aligned} P_c^{\text{SD}}(X) = &\, 0.38049 \left(\frac{m_c(m_c)}{1.30\text{ GeV}}\right)^{0.5081} \left(\frac{\alpha_s(M_Z)}{0.1176}\right)^{1.0192} \left(1 + \sum_{i,j} \kappa_{ij} L_{m_c}^i L_{\alpha_s}^j\right) \\ &\pm 0.008707 \left(\frac{m_c(m_c)}{1.30\text{ GeV}}\right)^{0.5276} \left(\frac{\alpha_s(M_Z)}{0.1176}\right)^{1.8970} \left(1 + \sum_{i,j} \epsilon_{ij} L_{m_c}^i L_{\alpha_s}^j\right), \end{aligned} \tag{B.1}$$

where

$$L_{m_c} = \ln\left(\frac{m_c(m_c)}{1.30\text{ GeV}}\right), \qquad L_{\alpha_s} = \ln\left(\frac{\alpha_s(M_Z)}{0.1176}\right) \tag{B.2}$$

and

$$\begin{aligned} &\kappa_{10} = 1.6624, \quad \kappa_{01} = -2.3537, \quad \kappa_{11} = -1.5862, \quad \kappa_{20} = 1.5036, \quad \kappa_{02} = -4.3477, \\ &\epsilon_{10} = -0.3537, \quad \epsilon_{01} = 0.6003, \quad \epsilon_{11} = -4.7652, \quad \epsilon_{20} = 1.0253, \quad \epsilon_{02} = 0.8866. \end{aligned} \tag{B.3}$$

JHEP11(2015)033

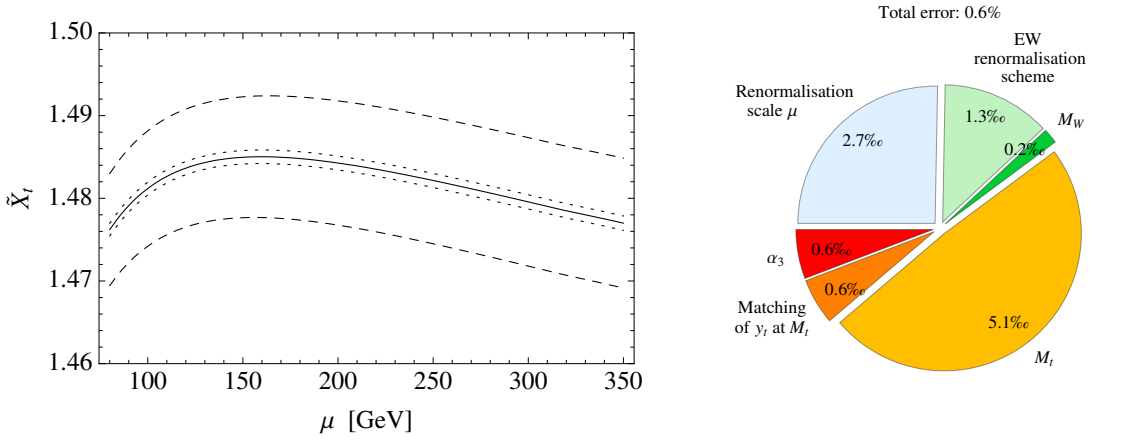

Figure 8. Left: renormalisation scale dependence of the quantity $\tilde{X}(\mu)$. The dashed lines show the uncertainty due to the error on the measured pole top mass M_t, while the dotted lines correspond to the theoretical error on the $\overline{\text{MS}}$ top Yukawa coupling y_t due to higher orders in the matching at the weak scale. Right: different sources of error affecting X_t.

C More details on ε'/ε

The basic one-loop functions entering (5.6) are given by (A.2) and

$$Y_0(x_t) = \frac{x_t}{8}\left[\frac{x_t-4}{x_t-1}+\frac{3x_t}{(x_t-1)^2}\ln x_t\right], \tag{C.1}$$

$$Z_0(x_t) = -\frac{1}{9}\ln x_t + \frac{18x_t^4-163x_t^3+259x_t^2-108x_t}{144(x_t-1)^3} + \\ + \frac{32x_t^4-38x_t^3-15x_t^2+18x_t}{72(x_t-1)^4}\ln x_t \tag{C.2}$$

$$E_0(x_t) = -\frac{2}{3}\ln x_t + \frac{x_t^2(15-16x_t+4x_t^2)}{6(1-x_t)^4}\ln x_t + \frac{x_t(18-11x_t-x_t^2)}{12(1-x_t)^3}, \tag{C.3}$$

where $x_t = m_t^2/M_W^2$.

The coefficients $r_i^{(0)}$, $r_i^{(6)}$ and $r_i^{(8)}$ entering (5.7) are given in the NDR renormalisation scheme for $\mu = m_c$ and three values of $\alpha_s(M_Z)$ in table 4.

The parameters $B_6^{(1/2)}$ and $B_8^{3/2}$ are related to the hadronic matrix elements Q_6 and Q_8 as follows

$$\langle Q_6(\mu)\rangle_0 = -4\left[\frac{m_{\rm K}^2}{m_s(\mu)+m_d(\mu)}\right]^2 (F_K - F_\pi)\, B_6^{(1/2)}, \tag{C.4}$$

$$\langle Q_8(\mu)\rangle_2 = \sqrt{2}\left[\frac{m_{\rm K}^2}{m_s(\mu)+m_d(\mu)}\right]^2 F_\pi\, B_8^{(3/2)}. \tag{C.5}$$

It should be emphasised that the overall factor in these expressions depends on the normalisation of the amplitudes $A_{0,2}$. The matrix elements given above correspond to the normalisation used in [23, 46, 93]. On the other hand the RBC-UKQCD collaboration [82, 94] uses

JHEP11(2015)033

	$\alpha_s(M_Z) = 0.1179$			$\alpha_s(M_Z) = 0.1185$			$\alpha_s(M_Z) = 0.1191$		
i	$r_i^{(0)}$	$r_i^{(6)}$	$r_i^{(8)}$	$r_i^{(0)}$	$r_i^{(6)}$	$r_i^{(8)}$	$r_i^{(0)}$	$r_i^{(6)}$	$r_i^{(8)}$
0	-3.392	15.293	1.271	-3.421	15.624	1.231	-3.451	15.967	1.191
X_0	0.655	0.029	0.	0.655	0.030	0.	0.655	0.031	0.
Y_0	0.451	0.114	0.	0.449	0.116	0.	0.447	0.118	0.
Z_0	0.406	-0.022	-13.435	0.420	-0.022	-13.649	0.435	-0.023	-13.872
E_0	0.229	-1.760	0.652	0.228	-1.788	0.665	0.226	-1.816	0.678

Table 4. The coefficients $r_i^{(0)}$, $r_i^{(6)}$ and $r_i^{(8)}$ of formula (5.7) in the NDR-$\overline{\text{MS}}$ scheme for three values of $\alpha_s(M_Z)$. From [83].

a different normalisation adopted in [91]. By comparing (C.4) and (C.5) with eqs. (5.10) and (5.18) of the latter paper we find that the matrix elements in [91] have and additional factor of $\sqrt{3/2}$. While ε'/ε clearly does not depend on this difference, it is crucial to take it into account when extracting the value of $B_8^{(3/2)}$ from the results obtained by RBC-UKQCD collaboration. To this end we use eq. (30) for A_2 in [94], adjust to our normalisation, and compare to A_2 expressed in terms of $\langle Q_8(\mu)\rangle_2$ in (C.5). This allows us to related $\langle Q_8(\mu)\rangle_2$ to the hadronic matrix element $\mathcal{M}_{(8,8)_{\text{mix}}}^{\overline{\text{MS}}-\text{NDR}}$ used in [82, 94]:

$$\langle Q_8(\mu)\rangle_2 = \frac{1}{3\sqrt{2}}\mathcal{M}_{(8,8)_{\text{mix}}}^{\overline{\text{MS}}-\text{NDR}} \tag{C.6}$$

In this manner we find

$$B_8^{(3/2)}(\mu) = \frac{1}{6F_\pi}\left[\frac{m_s(\mu)+m_d(\mu)}{m_{\text{K}}^2}\right]^2 \mathcal{M}_{(8,8)_{\text{mix}}}^{\overline{\text{MS}}-\text{NDR}}(\mu)\,. \tag{C.7}$$

The μ dependence of $\mathcal{M}_{(8,8)_{\text{mix}}}^{\overline{\text{MS}}-\text{NDR}}(\mu)$ is practically cancelled by the one of quark masses so that $B_8^{(3/2)}$ is practically μ-independent. In particular in the $\overline{\text{MS}}$-NDR scheme the μ-dependence is very weak [91].

Using the QCD lattice value from [82][8]

$$\mathcal{M}_{(8,8)_{\text{mix}}}^{\overline{\text{MS}}-\text{NDR}}(3\,\text{GeV}) = 4.55 \pm 0.27, \tag{C.8}$$

together with the light quark mass values [44]

$$m_s(2\,\text{GeV}) = (93.8 \pm 2.4)\,\text{MeV}, \qquad m_d(2\,\text{GeV}) = (4.68 \pm 0.16)\,\text{MeV}, \tag{C.9}$$

we find

$$B_8^{(3/2)}(3\,\text{GeV}) = 0.75 \pm 0.05, \qquad B_8^{(3/2)}(m_c) = 0.76 \pm 0.05. \tag{C.10}$$

[8] We thank Tadeusz Jankowski for translating the result in [82] into the $\overline{\text{MS}}$-NDR scheme.

JHEP11(2015)033

References

[1] G. Buchalla and A.J. Buras, *QCD corrections to rare K and B decays for arbitrary top quark mass*, *Nucl. Phys.* **B 400** (1993) 225 [INSPIRE].

[2] M. Misiak and J. Urban, *QCD corrections to FCNC decays mediated by Z penguins and W boxes*, *Phys. Lett.* **B 451** (1999) 161 [hep-ph/9901278] [INSPIRE].

[3] G. Buchalla and A.J. Buras, *The rare decays $K \to \pi\nu\bar{\nu}$, $B \to X\nu\bar{\nu}$ and $B \to \ell^+\ell^-$: An Update*, *Nucl. Phys.* **B 548** (1999) 309 [hep-ph/9901288] [INSPIRE].

[4] A.J. Buras, M. Gorbahn, U. Haisch and U. Nierste, *The Rare decay $K^+ \to \pi^+\nu\bar{\nu}$ at the next-to-next-to-leading order in QCD*, *Phys. Rev. Lett.* **95** (2005) 261805 [hep-ph/0508165] [INSPIRE].

[5] A.J. Buras, M. Gorbahn, U. Haisch and U. Nierste, *Charm quark contribution to $K^+ \to \pi^+\nu\bar{\nu}$ at next-to-next-to-leading order*, *JHEP* **11** (2006) 002 [*Erratum ibid.* **1211** (2012) 167] [hep-ph/0603079] [INSPIRE].

[6] M. Gorbahn and U. Haisch, *Effective Hamiltonian for non-leptonic $|\Delta F| = 1$ decays at NNLO in QCD*, *Nucl. Phys.* **B 713** (2005) 291 [hep-ph/0411071] [INSPIRE].

[7] J. Brod and M. Gorbahn, *Electroweak Corrections to the Charm Quark Contribution to $K^+ \to \pi^+\nu\bar{\nu}$*, *Phys. Rev.* **D 78** (2008) 034006 [arXiv:0805.4119] [INSPIRE].

[8] J. Brod, M. Gorbahn and E. Stamou, *Two-Loop Electroweak Corrections for the $K \to \pi\nu\bar{\nu}$ Decays*, *Phys. Rev.* **D 83** (2011) 034030 [arXiv:1009.0947] [INSPIRE].

[9] G. Buchalla and A.J. Buras, *Two loop large m_t electroweak corrections to $K \to \pi\nu\bar{\nu}$ for arbitrary Higgs boson mass*, *Phys. Rev.* **D 57** (1998) 216 [hep-ph/9707243] [INSPIRE].

[10] G. Isidori, F. Mescia and C. Smith, *Light-quark loops in $K \to \pi\nu\bar{\nu}$*, *Nucl. Phys.* **B 718** (2005) 319 [hep-ph/0503107] [INSPIRE].

[11] F. Mescia and C. Smith, *Improved estimates of rare K decay matrix-elements from $K_{\ell 3}$ decays*, *Phys. Rev.* **D 76** (2007) 034017 [arXiv:0705.2025] [INSPIRE].

[12] A.J. Buras, F. Schwab and S. Uhlig, *Waiting for precise measurements of $K^+ \to \pi^+\nu\bar{\nu}$ and $K_L \to \pi^0\nu\bar{\nu}$*, *Rev. Mod. Phys.* **80** (2008) 965 [hep-ph/0405132] [INSPIRE].

[13] G. Isidori, *Flavor Physics with light quarks and leptons*, *eConf* **C 060409** (2006) 035 [hep-ph/0606047] [INSPIRE].

[14] C. Smith, *Theory review on rare K decays: Standard model and beyond*, hep-ph/0608343 [INSPIRE].

[15] T.K. Komatsubara, *Experiments with K-Meson Decays*, *Prog. Part. Nucl. Phys.* **67** (2012) 995 [arXiv:1203.6437] [INSPIRE].

[16] A.J. Buras and J. Girrbach, *Towards the Identification of New Physics through Quark Flavour Violating Processes*, *Rept. Prog. Phys.* **77** (2014) 086201 [arXiv:1306.3775] [INSPIRE].

[17] M. Blanke, *New Physics Signatures in Kaon Decays*, *PoS* **KAON13** (2013) 010 [arXiv:1305.5671] [INSPIRE].

[18] C. Smith, *Rare K decays: Challenges and Perspectives*, arXiv:1409.6162 [INSPIRE].

[19] A.J. Buras, D. Buttazzo, J. Girrbach-Noe and R. Knegjens, *Can we reach the Zeptouniverse with rare K and $B_{s,d}$ decays?*, *JHEP* **11** (2014) 121 [arXiv:1408.0728] [INSPIRE].

JHEP11(2015)033

[20] F. Newson et al., *Prospects for $K^+ \to \pi^+ \nu\bar{\nu}$ at CERN in NA62*, arXiv:1411.0109 [INSPIRE].

[21] A. Romano, *The $K^+ \to \pi^+ \nu\bar{\nu}$ decay in the NA62 experiment at CERN*, arXiv:1411.6546 [INSPIRE].

[22] KOTO collaboration, K. Shiomi, *$K_L^0 \to \pi^0 \nu\bar{\nu}$ at KOTO*, arXiv:1411.4250 [INSPIRE].

[23] A.J. Buras, F. De Fazio and J. Girrbach, *$\Delta I = 1/2$ rule, ε'/ε and $K \to \pi\nu\bar{\nu}$ in $Z'(Z)$ and G' models with FCNC quark couplings*, *Eur. Phys. J.* **C 74** (2014) 2950 [arXiv:1404.3824] [INSPIRE].

[24] C. Bobeth, U. Haisch, A. Lenz, B. Pecjak and G. Tetlalmatzi-Xolocotzi, *On new physics in $\Delta\Gamma_d$*, *JHEP* **06** (2014) 040 [arXiv:1404.2531] [INSPIRE].

[25] C. Bobeth, M. Gorbahn and S. Vickers, *Weak annihilation and new physics in charmless $B \to MM$ decays*, *Eur. Phys. J.* **C 75** (2015) 340 [arXiv:1409.3252] [INSPIRE].

[26] J. Brod, A. Lenz, G. Tetlalmatzi-Xolocotzi and M. Wiebusch, *New physics effects in tree-level decays and the precision in the determination of the quark mixing angle γ*, *Phys. Rev.* **D 92** (2015) 033002 [arXiv:1412.1446] [INSPIRE].

[27] UTfit collaboration, M. Bona et al., *The Unitarity Triangle Fit in the Standard Model and Hadronic Parameters from Lattice QCD: A Reappraisal after the Measurements of $\Delta m(s)$ and $BR(B \to \tau\nu_\tau)$*, *JHEP* **10** (2006) 081 [hep-ph/0606167] [INSPIRE].

[28] J. Charles et al., *Current status of the Standard Model CKM fit and constraints on $\Delta F = 2$ New Physics*, *Phys. Rev.* **D 91** (2015) 073007 [arXiv:1501.05013] [INSPIRE].

[29] S.H. Kettell, L.G. Landsberg and H.H. Nguyen, *Alternative technique for standard model estimation of the rare kaon decay branchings $BR(K \to \pi\nu\bar{\nu})$ (SM)*, *Phys. Atom. Nucl.* **67** (2004) 1398 [hep-ph/0212321] [INSPIRE].

[30] A.J. Buras and J. Girrbach, *Stringent tests of constrained Minimal Flavor Violation through $\Delta F = 2$ transitions*, *Eur. Phys. J.* **C 73** (2013) 2560 [arXiv:1304.6835] [INSPIRE].

[31] Fermilab Lattice, MILC collaboration, C.M. Bouchard et al., *Neutral B-Meson Mixing Parameters in and beyond the SM with 2+1 Flavor Lattice QCD*, *PoS* **LATTICE2014** (2014) 378 [arXiv:1412.5097] [INSPIRE].

[32] Fermilab Lattice, MILC collaborations, D. Du et al., *$B \to \pi\ell\nu$ semileptonic form factors from unquenched lattice QCD and determination of $|V_{ub}|$*, *PoS* **LATTICE2014** (2014) 385 [arXiv:1411.6038] [INSPIRE].

[33] A.J. Buras, *Weak Hamiltonian, CP-violation and rare decays*, hep-ph/9806471 [INSPIRE].

[34] D. Buttazzo, G. Degrassi, P.P. Giardino, G.F. Giudice, F. Sala, A. Salvio et al., *Investigating the near-criticality of the Higgs boson*, *JHEP* **12** (2013) 089 [arXiv:1307.3536] [INSPIRE].

[35] G. Isidori, G. Martinelli and P. Turchetti, *Rare kaon decays on the lattice*, *Phys. Lett.* **B 633** (2006) 75 [hep-lat/0506026] [INSPIRE].

[36] G. Buchalla and A.J. Buras, *The rare decays $K^+ \to \pi^+ \nu\bar{\nu}$ and $K_L \to \mu^+\mu^-$ beyond leading logarithms*, *Nucl. Phys.* **B 412** (1994) 106 [hep-ph/9308272] [INSPIRE].

[37] K.G. Chetyrkin, J.H. Kuhn, A. Maier, P. Maierhofer, P. Marquard et al., *Charm and Bottom Quark Masses: An Update*, *Phys. Rev.* **D 80** (2009) 074010 [arXiv:0907.2110] [INSPIRE].

[38] Particle Data Group collaboration, J. Beringer et al., *Review of Particle Physics (RPP)*, *Phys. Rev.* **D 86** (2012) 010001 [INSPIRE].

JHEP11(2015)033

[39] G. Buchalla and A.J. Buras, *$K \to \pi\nu\bar{\nu}$ and high precision determinations of the CKM matrix*, *Phys. Rev.* **D 54** (1996) 6782 [hep-ph/9607447] [INSPIRE].

[40] G. Buchalla, A.J. Buras and M.E. Lautenbacher, *Weak decays beyond leading logarithms*, *Rev. Mod. Phys.* **68** (1996) 1125 [hep-ph/9512380] [INSPIRE].

[41] E949 collaboration, A.V. Artamonov et al., *New measurement of the $K^+ \to \pi^+\nu\bar{\nu}$ branching ratio*, *Phys. Rev. Lett.* **101** (2008) 191802 [arXiv:0808.2459] [INSPIRE].

[42] E391A collaboration, J.K. Ahn et al., *Experimental study of the decay $K_L^0 \to \pi^0\nu\bar{\nu}$*, *Phys. Rev.* **D 81** (2010) 072004 [arXiv:0911.4789] [INSPIRE].

[43] ORKA collaboration, E.T. Worcester, *ORKA, The Golden Kaon Experiment: Precision measurement of $K^+ \to \pi^+\nu\bar{\nu}$ and other rare processes*, *PoS* **KAON13** (2013) 035 [arXiv:1305.7245] [INSPIRE].

[44] S. Aoki et al., *Review of lattice results concerning low-energy particle physics*, *Eur. Phys. J.* **C 74** (2014) 2890 [arXiv:1310.8555] [INSPIRE].

[45] Heavy Flavor Averaging Group collaboration, Y. Amhis et al., *Averages of B-Hadron, C-Hadron and tau-lepton properties as of early 2012*, arXiv:1207.1158 [INSPIRE].

[46] A.J. Buras, J.-M. Gérard and W.A. Bardeen, *Large-N Approach to Kaon Decays and Mixing 28 Years Later: $\Delta I = 1/2$ Rule, $\hat{B}_K$ and ΔM_K*, *Eur. Phys. J.* **C 74** (2014) 2871 [arXiv:1401.1385] [INSPIRE].

[47] K. Trabelsi, on behalf of the CKMfitter Group collaboration, *World average and experimental overview of γ/φ_3*, presented at CKM 2014, http://ckmfitter.in2p3.fr.

[48] J. Brod and M. Gorbahn, *Next-to-Next-to-Leading-Order Charm-Quark Contribution to the CP-violation Parameter ε_K and ΔM_K*, *Phys. Rev. Lett.* **108** (2012) 121801 [arXiv:1108.2036] [INSPIRE].

[49] J. Brod and M. Gorbahn, *ε_K at Next-to-Next-to-Leading Order: The Charm-Top-Quark Contribution*, *Phys. Rev.* **D 82** (2010) 094026 [arXiv:1007.0684] [INSPIRE].

[50] A.J. Buras, M. Jamin and P.H. Weisz, *Leading and Next-to-leading QCD Corrections to ε Parameter and $B^0 - \bar{B}^0$ Mixing in the Presence of a Heavy Top Quark*, *Nucl. Phys.* **B 347** (1990) 491 [INSPIRE].

[51] J. Urban, F. Krauss, U. Jentschura and G. Soff, *Next-to-leading order QCD corrections for the $B^0 - \bar{B}^0$ mixing with an extended Higgs sector*, *Nucl. Phys.* **B 523** (1998) 40 [hep-ph/9710245] [INSPIRE].

[52] ATLAS, CDF, CMS, D0 collaborations, *First combination of Tevatron and LHC measurements of the top-quark mass*, arXiv:1403.4427 [INSPIRE].

[53] G. Ricciardi, *Status of $|V_{cb}|$ and $|V_{ub}|$ CKM matrix elements*, arXiv:1412.4288 [INSPIRE].

[54] G. Ricciardi, *Determination of the CKM matrix elements $|V_{xb}|$*, *Mod. Phys. Lett.* **A 28** (2013) 1330016 [arXiv:1305.2844] [INSPIRE].

[55] P. Gambino, *Inclusive semileptonic B decays and $|V_{cb}|$: In memoriam Kolya Uraltsev*, *Int. J. Mod. Phys.* **A 30** (2015) 1543002 [arXiv:1501.00314] [INSPIRE].

[56] Fermilab Lattice, MILC collaborations, J.A. Bailey et al., *Update of $|V_{cb}|$ from the $\bar{B} \to D^*\ell\bar{\nu}$ form factor at zero recoil with three-flavor lattice QCD*, *Phys. Rev.* **D 89** (2014) 114504 [arXiv:1403.0635] [INSPIRE].

JHEP11(2015)033

[57] A. Alberti, P. Gambino, K.J. Healey and S. Nandi, *Precision Determination of the Cabibbo-Kobayashi-Maskawa Element V_{cb}*, *Phys. Rev. Lett.* **114** (2015) 061802 [arXiv:1411.6560] [INSPIRE].

[58] S. Descotes-Genon, J. Matias and J. Virto, *An analysis of $B_{d,s}$ mixing angles in presence of New Physics and an update of $B_s \to K^{0*}\bar{K}^{0*}$*, *Phys. Rev.* **D 85** (2012) 034010 [arXiv:1111.4882] [INSPIRE].

[59] K. De Bruyn, R. Fleischer, R. Knegjens, P. Koppenburg, M. Merk and N. Tuning, *Branching Ratio Measurements of B_s Decays*, *Phys. Rev.* **D 86** (2012) 014027 [arXiv:1204.1735] [INSPIRE].

[60] K. De Bruyn, R. Fleischer, R. Knegjens, P. Koppenburg, M. Merk et al., *Probing New Physics via the $B_s^0 \to \mu^+\mu^-$ Effective Lifetime*, *Phys. Rev. Lett.* **109** (2012) 041801 [arXiv:1204.1737] [INSPIRE].

[61] G. D'Ambrosio, G.F. Giudice, G. Isidori and A. Strumia, *Minimal flavor violation: An Effective field theory approach*, *Nucl. Phys.* **B 645** (2002) 155 [hep-ph/0207036] [INSPIRE].

[62] A.J. Buras, P. Gambino, M. Gorbahn, S. Jager and L. Silvestrini, *Universal unitarity triangle and physics beyond the standard model*, *Phys. Lett.* **B 500** (2001) 161 [hep-ph/0007085] [INSPIRE].

[63] G. Buchalla and A.J. Buras, *$\sin 2\beta$ from $K \to \pi\nu\bar{\nu}$*, *Phys. Lett.* **B 333** (1994) 221 [hep-ph/9405259] [INSPIRE].

[64] A.J. Buras and R. Fleischer, *Bounds on the unitarity triangle, $\sin 2\beta$ and $K \to \pi\nu\bar{\nu}$ decays in models with minimal flavor violation*, *Phys. Rev.* **D 64** (2001) 115010 [hep-ph/0104238] [INSPIRE].

[65] S. Faller, M. Jung, R. Fleischer and T. Mannel, *The Golden Modes $B^0 \to J/\psi K_{S,L}$ in the Era of Precision Flavour Physics*, *Phys. Rev.* **D 79** (2009) 014030 [arXiv:0809.0842] [INSPIRE].

[66] A.J. Buras, *Relations between $\Delta M_{s,d}$ and $B_{s,d} \to \mu^+\mu^-$ in models with minimal flavor violation*, *Phys. Lett.* **B 566** (2003) 115 [hep-ph/0303060] [INSPIRE].

[67] R. Barbieri, D. Buttazzo, F. Sala and D.M. Straub, *Flavour physics from an approximate $U(2)^3$ symmetry*, *JHEP* **07** (2012) 181 [arXiv:1203.4218] [INSPIRE].

[68] A.J. Buras and D. Guadagnoli, *Correlations among new CP-violating effects in $\Delta F = 2$ observables*, *Phys. Rev.* **D 78** (2008) 033005 [arXiv:0805.3887] [INSPIRE].

[69] A.J. Buras, D. Guadagnoli and G. Isidori, *On ε_K Beyond Lowest Order in the Operator Product Expansion*, *Phys. Lett.* **B 688** (2010) 309 [arXiv:1002.3612] [INSPIRE].

[70] A. Caldwell, D. Kollar and K. Kroninger, *BAT: The Bayesian Analysis Toolkit*, *Comput. Phys. Commun.* **180** (2009) 2197 [arXiv:0808.2552] [INSPIRE].

[71] C. Bobeth, M. Gorbahn, T. Hermann, M. Misiak, E. Stamou and M. Steinhauser, *$B_{s,d} \to \ell^+\ell^-$ in the Standard Model with Reduced Theoretical Uncertainty*, *Phys. Rev. Lett.* **112** (2014) 101801 [arXiv:1311.0903] [INSPIRE].

[72] LHCb, CMS collaborations, V. Khachatryan et al., *Observation of the rare $B_s^0 \to \mu^+\mu^-$ decay from the combined analysis of CMS and LHCb data*, *Nature* **522** (2015) 68 [arXiv:1411.4413] [INSPIRE].

[73] G. D'Ambrosio and G. Isidori, *$K^+ \to \pi^+\nu\bar{\nu}$: A Rising star on the stage of flavor physics*, *Phys. Lett.* **B 530** (2002) 108 [hep-ph/0112135] [INSPIRE].

JHEP11(2015)033

[74] NA48 collaboration, J.R. Batley et al., *A Precision measurement of direct CP-violation in the decay of neutral kaons into two pions*, *Phys. Lett.* **B 544** (2002) 97 [hep-ex/0208009] [INSPIRE].

[75] KTeV collaboration, A. Alavi-Harati et al., *Measurements of direct CP-violation, CPT symmetry and other parameters in the neutral kaon system*, *Phys. Rev.* **D 67** (2003) 012005 [*Erratum ibid.* **D 70** (2004) 079904] [hep-ex/0208007] [INSPIRE].

[76] KTeV collaboration, E.T. Worcester, *The Final Measurement of ε'/ε from KTeV*, arXiv:0909.2555 [INSPIRE].

[77] A.J. Buras and J.M. Gérard, *$1/N$ Expansion for Kaons*, *Nucl. Phys.* **B 264** (1986) 371 [INSPIRE].

[78] W.A. Bardeen, A.J. Buras and J.M. Gérard, *The $\Delta I = 1/2$ Rule in the Large-N Limit*, *Phys. Lett.* **B 180** (1986) 133 [INSPIRE].

[79] A.J. Buras and J.M. Gérard, *Isospin Breaking Contributions to ε'/ε*, *Phys. Lett.* **B 192** (1987) 156 [INSPIRE].

[80] T. Hambye, G.O. Kohler, E.A. Paschos, P.H. Soldan and W.A. Bardeen, *$1/N$ corrections to the hadronic matrix elements of Q_6 and Q_8 in $K \to \pi\pi$ decays*, *Phys. Rev.* **D 58** (1998) 014017 [hep-ph/9802300] [INSPIRE].

[81] Z. Bai et al., *Standard-model prediction for direct CP-violation in $K \to \pi\pi$ decay*, arXiv:1505.07863 [INSPIRE].

[82] T. Blum et al., *$K \to \pi\pi$ $\Delta I = 3/2$ decay amplitude in the continuum limit*, *Phys. Rev.* **D 91** (2015) 074502 [arXiv:1502.00263] [INSPIRE].

[83] A.J. Buras, M. Gorbahn, S. äger and M. Jamin, *Improved anatomy of ε'/ε in the Standard Model*, arXiv:1507.06345 [INSPIRE].

[84] A.J. Buras and J.-M. Gérard, *Upper Bounds on ε'/ε Parameters $B_6^{(1/2)}$ and $B_8^{(3/2)}$ from Large-N QCD and other News*, arXiv:1507.06326 [INSPIRE].

[85] A.J. Buras and L. Silvestrini, *Upper bounds on $K \to \pi\nu\bar{\nu}$ and $K_L \to \pi^0 e^+ e^-$ from ε'/ε and $K_L \to \mu^+\mu^-$*, *Nucl. Phys.* **B 546** (1999) 299 [hep-ph/9811471] [INSPIRE].

[86] A.J. Buras, G. Colangelo, G. Isidori, A. Romanino and L. Silvestrini, *Connections between ε'/ε and rare kaon decays in supersymmetry*, *Nucl. Phys.* **B 566** (2000) 3 [hep-ph/9908371] [INSPIRE].

[87] M. Blanke, A.J. Buras, S. Recksiegel, C. Tarantino and S. Uhlig, *Correlations between ε'/ε and rare K decays in the littlest Higgs model with T-parity*, *JHEP* **06** (2007) 082 [arXiv:0704.3329] [INSPIRE].

[88] M. Bauer, S. Casagrande, U. Haisch and M. Neubert, *Flavor Physics in the Randall-Sundrum Model: II. Tree-Level Weak-Interaction Processes*, *JHEP* **09** (2010) 017 [arXiv:0912.1625] [INSPIRE].

[89] A.J. Buras, D. Buttazzo and R. Knegjens, *$K \to \pi\nu\bar{\nu}$ and ε'/ε in Simplified New Physics Models*, arXiv:1507.08672 [INSPIRE].

[90] M. Blanke, A.J. Buras and S. Recksiegel, *Quark flavour observables in the Littlest Higgs model with T-parity after LHC Run 1*, arXiv:1507.06316 [INSPIRE].

[91] A.J. Buras, M. Jamin and M.E. Lautenbacher, *The Anatomy of ε'/ε beyond leading logarithms with improved hadronic matrix elements*, *Nucl. Phys.* **B 408** (1993) 209 [hep-ph/9303284] [INSPIRE].

JHEP11(2015)033

[92] A.J. Buras, J. Girrbach-Noe, C. Niehoff and D.M. Straub, $B \to K^{(*)}\nu\overline{\nu}$ *decays in the Standard Model and beyond*, *JHEP* **02** (2015) 184 [arXiv:1409.4557] [INSPIRE].

[93] V. Cirigliano, G. Ecker, H. Neufeld, A. Pich and J. Portoles, *Kaon Decays in the Standard Model*, *Rev. Mod. Phys.* **84** (2012) 399 [arXiv:1107.6001] [INSPIRE].

[94] T. Blum et al., *Lattice determination of the* $K \to (\pi\pi)_{I=2}$ *Decay Amplitude* A_2, *Phys. Rev.* **D 86** (2012) 074513 [arXiv:1206.5142] [INSPIRE].

JHEP11(2015)033